universität wien

MASTERARBEIT / MASTER'S THESIS

A new broad-scale assessment method for combined effects of climate change and nitrogen deposition on habitats

verfasst von / submitted by

Anna Ida Hämmerle, B.Sc.

angestrebter akademischer Grad / in partial fulfilment of the requirements for the degree of

Master of Science (M.Sc.)

Wien, 2016

Studienkennzahl:	A 066 879
Studienrichtung:	Naturschutz und Biodiversitätsmanagement / Nature Conservation and Biodiversity Management
Betreut von:	Univ.-Prof. Mag. Dr. Stefan Dullinger

Danksagung

Ich möchte allen meinen Lieben danken, die ein offenes Ohr für meine Sorgen und Nöte hatten, wann immer ich den Kopf in den Sand stecken wollte. Mal ein Wort des Zuspruchs, mal eine Umarmung, mal einfach nur ablenken. Ich danke euch herzlich – euch allen die das letzte Jahr über an meiner Seite standen ob nah oder fern.

Danken möchte ich auch Stefan und Thomas, dafür dass ihr mir das Thema anvertraut habt, eure Leitung und Betreuung.

Ganz besonderer Dank gilt Johannes. Ohne dich würde ich vermutlich heute noch an der Arbeit sitzen. Du bist ein wunderbarer Lehrer, stets geduldig und bereit zu helfen. Zu wissen, dass ich immer zu dir kommen konnte, wenn ich nicht weiter wusste, dass du dir Zeit genommen hast, selbst wenn du selber bis oben hin in Arbeit gesteckt hast und dafür dass ich so vieles von dir lernen konnte, dafür danke ich dir.

Table of Contents

Abstract

Climate change and nitrogen (N) deposition are among the most important determinants of changes in biodiversity at a global scale and are interlinked, although commonly considered separately in applied research, conservation, and policy development. Both empirical and modelling studies indicate that in concert climate change and nitrogen deposition may trigger a more pronounced biodiversity loss than each stressor alone. Interactive effects thus need to be considered in conservation strategies. In this study we propose a method for broad scale risk assessment employing standard procedures such as climate envelope modelling and the evaluation of exceedances of empirical Critical Loads for eutrophication through N deposition. A combined habitat-specific risk metric is calculated, which is the scaled exceedance of the N critical load and climatic thresholds in the three dimensional space of temperature, water limitation and nitrogen deposition. Projected into geographical space, risk maps for the Austrian territory, for both current and future climatic and nitrogen deposition scenarios, indicated high combined impact on abundant habitats such as coniferous woodlands and disproportional high risk to alpine habitats. We propose this method as a tool that might support the prioritization and guidance of conservation strategies.

Zusammenfassung

Global gesehen sind Klimawandel und Stickstoffdeposition zwei der wichtigsten Gefährdungsfaktoren für Biodiversität und eng miteinander verknüpft. Dennoch werden sie in angewandter Wissenschaft sowie Natur- und Umweltschutz-Strategien und -Maßnahmen meist getrennt behandelt. Empirische Studien und Modellierungen indizieren jedoch eine potentiell beträchtliche negative interaktive Wirkung. Mit dieser Studie möchten wir eine neue Methode für die Risikoanalyse von Habitaten vorstellen, die Gefährdung durch Klimawandel und Stickstoffeintrag in eine Maßzahl zusammenfasst. Diese Maßzahl wird aus der skalierten Überschreitung kritischer klimatischer und Stickstoff-Schwellenwerte errechnet. Mithilfe von Artverbreitungsmodellierungen und kritischen Schwellenwerten für Stickstoffdeposition (engl. Critical load) kann sie Habitat-spezifisch und räumlich explizit dargestellt werden. Wir illustrieren die Methode mit Gefährdungskarten für Österreich unter aktuellen und zukünftigen Klima- und Stickstoffdepositionsszenarien. Die Ergebnisse zeigen hohe Risiken durch kombinierte Klima und N-Depostions-Effekte für weitverbreitete Habitate wie Koniferenwälder und ein überproportional hohes Risiko für alpine Habitate. Wir schlagen diese Methode für Prioritätensetzung und Strategientwicklung im Natur- und Umweltschutz vor.

1. Introduction

Climate change and nitrogen deposition are among the most important determinants of changes in biodiversity at a global scale (Millennium Ecosystem Assessment, 2005; Sala et al., 2000). The multiple components of climate change are anticipated to affect all levels of biodiversity, from organisms to biomes (Bellard et al., 2012). Predictions of responses on these different levels have been conducted repeatedly (Bellard et al., 2012; Dillon et al. 2010; Parmesan, 2006; Pereira et al., 2010) and play an important role in alerting scientists and policy makers to potential future risks.

Atmospheric nitrogen deposition, on the other hand, has increased substantially in the second half of the 20th century (Galloway et al., 2004) due to agricultural intensification and rising emissions from fossil fuel combustion. Among its numerous negative effects, N deposition drives eutrophication and acidification (via nitrification) of soils and causes loss of species richness and changes in species composition of terrestrial ecosystems (Bobbink et al., 2010; Dirnböck et al., 2014; McClean et al., 2011; Simkin et al., 2016; Stevens et al., 2010). Efforts have been made to define critical loads (CL) of nitrogen deposition for different types of ecosystems, i.e. thresholds beyond which negative effects are to be expected in the long run (Bobbink et al., 2010; Pardo et al., 2011). Among these negative effects is a change in their characteristic species composition.

Although commonly considered separately in applied research and policies, climate change and air pollution are interlinked (De Marco et al., 2014; de Vries & Posch, 2011; McDonnell et al., 2014). Climate influences atmospheric N deposition (through precipitation), as well as soil biogeochemistry. Temperature and moisture conditions control soil N availability as they are major drivers of litter decomposition (Butler et al., 2012; Guntiñas et al., 2012). Although interactions are complex, both empirical and modelling studies indicate that in concert climate change and nitrogen deposition may trigger a more pronounced biodiversity loss than each stressor alone (Porter et al., 2012; Zavaleta et al. 2003). On the other hand, dry and wet climate can also render plant communities insensitive to N deposition, as recently shown in a continental study (Simkin et al., 2016).

In this study we propose a new method to map future areas at risk of these potentially interacting effects. We adopted the critical load method, which is commonly used to assess the magnitude of risks from air pollutants (Posch et al. 2001), to additionally assess the risk of habitats caused by climate change. With species distribution modelling, also known as climate envelope-modelling, and an adaptation to the approach of stacking projections of individual characteristic plant species of a habitat, in order to predict its fate under differing environmental condition (Guisan & Rahbek, 2011), we were able to define critical, habitat-specific thresholds of climate warming and water limitation. The "exceedance" of the critical climate thresholds were numerically combined with the exceedance of the empirical critical load for N deposition. As an example, we applied the method to the territory of Austria by using climate and N deposition scenarios until 2050.

2. Material and Methods

2.1. Study area

The study area covers Austria, a land-locked country of central Europe spanning approximately 84,000 km². The mean annual temperature in Austria ranges between -9°C at the highest peaks of the Alps and 10° C in the Eastern lowlands, and the annual precipitation sum between a minimum of approximately 500 mm and a maximum of 2100 mm (www.worldclim.org). High climatic diversity is mainly due to the rugged terrain of the Austrian Alps, which cover about two thirds of the country, and drives considerable habitat diversity.

2.2. *Climatic data*

Spatial variability of current climatic conditions in Austria was mapped on a 100 x 100 m raster by statistically downscaling WorldClim maps (www.worlclim.org), original resolution 30 seconds ~ 1 km² in Austria) of monthly temperatures and precipitation sums to this spatial resolution. Downscaling was done by means of the so-called 'delta-method' (Dullinger et al., 2012; Zimmermann et al., 2009). Subsequently we calculated the mean annual temperature and annual precipitation sum for each cell of the 100 x 100 m raster.

Maps of the same two climatic variables were calculated for two scenarios of the most recent IPCC report (IPCC 2014), the representative concentration pathways RCP2.6 and RCP8.5, corresponding to the mildest and most severe climate change scenario, respectively. Maps of these climatic scenarios for the years 2030 (average 2014 – 2046) and 2050 (average 2034 – 2066) were taken from the Cordex portal (http://cordexesg.dmi.dk/esgf-web-fe/live) and downscaled to 100 x 100 m raster maps of future mean annual temperature and annual precipitation sums using the same procedures as applied to current climatic data.

2.3. Selection of habitat types

Critical loads are defined for specific habitat types. As our focus is on biodiversity conservation issues, we concentrated on natural and semi-natural habitat types of Austria in this study, and particularly disregarded agricultural fields, intensively used meadows and pastures as well as urban ecosystems. Classification of the focal habitat types was based on the syntaxonomical system of Austrian plant communities (Grabherr & Mucina, 1993; Willner & Grabherr, 2007). Overall, 66 “alliances” of this system were selected which represent various types of mires, mire forests, heaths, alpine grasslands, dry, wet and extensively used mesic grasslands, broad-leaved forests, and conifer forests (Appendix: Tab.1).

2.4. Species selection

“Alliances” and other classification levels of the syntaxonomical system represent plant community types which are essentially defined by particular combinations of diagnostic species (Rodwell et al., 2002), i.e. species, which are (largely) restricted to the respective syntaxonomical unit (Willner et al., 2009). Our approach is based on this concept by defining critical climatic thresholds of a particular community type (= habitat type, in this study) from an overlay of the climatic niches of its diagnostic species. These climatic niches are derived from species distribution models. We therefore extracted the full list of the diagnostic species of all 66 alliances from Grabherr & Mucina (1993) and Willner & Grabherr (2007).

2.5. Species distribution data

To cover the climatic niches of the diagnostic species as complete as possible we collected a set of 70780 vegetation samples covering most of central and parts of eastern, western and southern Europe. Samples represent complete lists of vascular plants growing in plots of variable sites (~ 5-500 m²). The data were provided by databases participating in the European Vegetation Archive (EVA) (Chytrý et al., 2016). All relevés were geo-referenced, mostly at an accuracy of < 1 km.

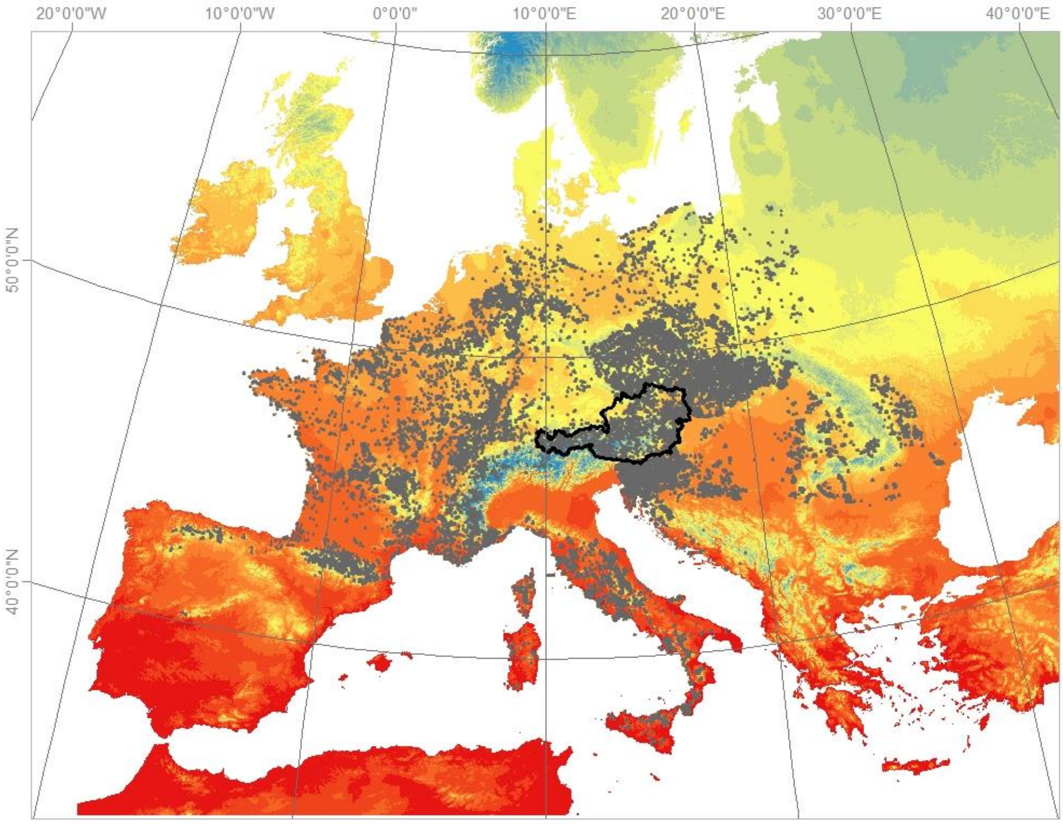

Fig.1 Climate variable bio1 (mean annual temperature) as base map, grey dots as sites of vegetation relevés and Austrian border indicated by black line

2.6. Species distribution models (SDM)

Species distribution models were fit by a selection of 482 diagnostic species which were sufficiently frequent (> 20 occurrences) in the 70,780 vegetation plots (Baatar et al., 2016, unpubl.). Models used presence-absence of a species in the plots as the dependent and mean annual temperature and annual precipitation sum as the independent variables. As the spatial accuracy of the plots was mostly > 1 km, but often lower than 100 x 100 m, we used the original 30''-WorldClim data for model fitting. SDMs were calibrated in biomod2 (Thuiller et al., 2012) using Generalized Linear Models (GLM), Generalized Boosted Regression Models (GBM), Generalized Additive Models (GAM) and Multivariate adaptive regression splines (MARS) with three replicate runs for each technique. In each run, a randomly selected subset of 70% of the plots was used for calibration and the remaining 30% for model evaluation. Fitted models were then used to project each species probability of occurrence into the two-dimensional climatic space using an ensemble forecasting approach. Thereby, the projected probability of occurrence at a particular combination of mean annual temperature and annual precipitation sum represents a weighted average of the projections of each single model, with ROC-scores of the models used as weights. Models with a ROC-score < 0.7 were excluded from the ensemble forecast (Appendix: Tab.2).

2.7. Niche models of alliances

Projected two-dimensional niches of all the diagnostic species of one community were subsequently stacked and occurrence probabilities averaged (cf. Fig. 2). For further analyses, we defined an average occurrence probability of 0.8 as the critical climatic threshold of the respective community. This threshold is the equivalent to the Critical Load of nitrogen deposition and controls how conservative or sensitive the resulting risk metric will be. We here used 0.8 as this value resulted in niche margins that we deemed realistic for the majority of alliances. We note, in addition, that the use of a relative scale in final metrics (see below) reduces the impact that threshold selection has on results.

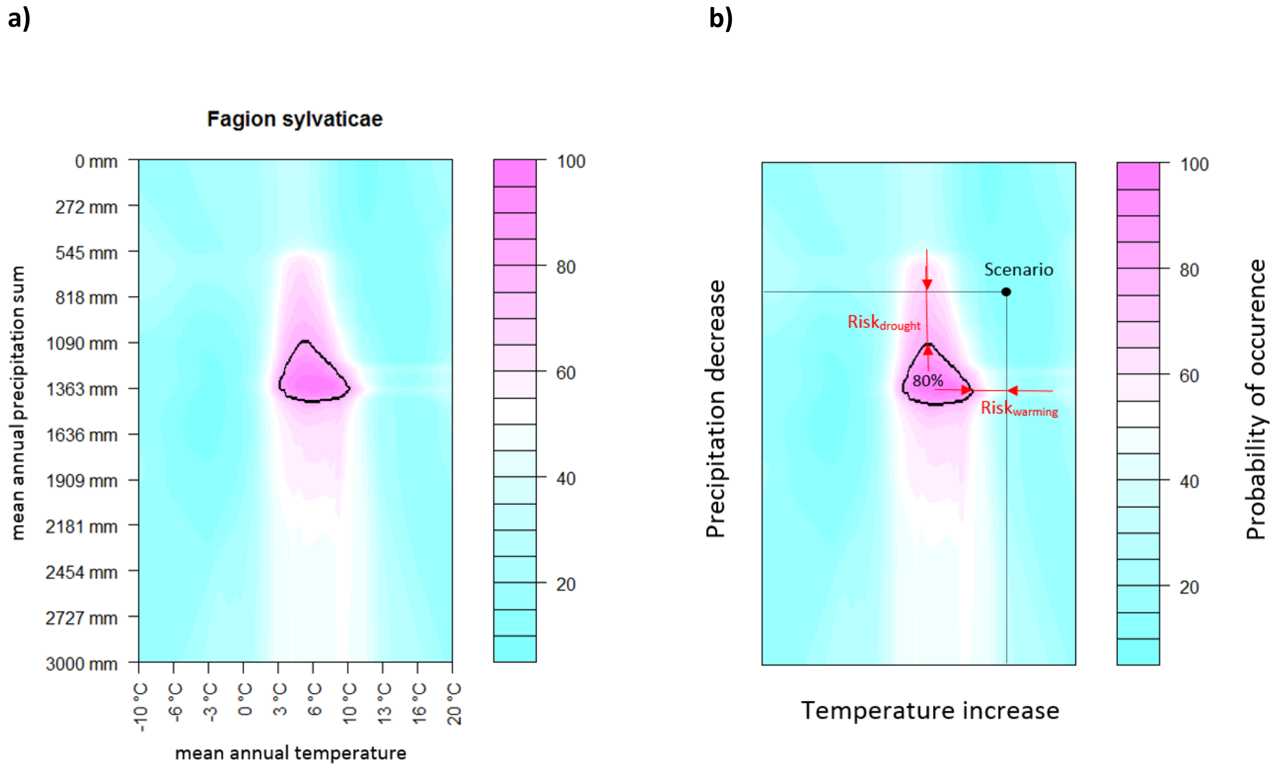

Fig.2 a) Representation of plant community niche in temperature / precipitation space (example: Fagion slyvaticae = European beech forests). Colours represent probability of occurrence as calculated from averaging SDM-projections of all diagnostic plant species of the community. The black line delimits the niche as defined by an averaged probability of occurrence of constituent species <= 0.8. The precipitation axis was reversed as we assumed drought stress to represent the main challenge for Austrian plants under climate change (Appendix: Tab.3)

b) Derivation of combined risk of plant communities from climate change schematically exemplified. Risk from N deposition is given by the exceedance of the critical load ($Risk_N$= Deposition – CL)

2.8. Data on N deposition

We downscaled existing EMEP-MSCW N deposition data (Simpson et al., 2012) with a resolution of 50 x 50 km to 0.1 x 0.05° Lat/Lon resolution using precipitation data and a digital elevation model. Precipitation was taken from Isotta et al. (2014), a daily precipitation dataset for the Alpine region (resolution 5 x 5 km). Annual mean precipitation sum for the period 1979 to 2008 was calculated from this data and spatially interpolated to the 0.1 x 0.05° Lat/Lon target resolution. The mean altitude of each cell of the 0.1 x 0.05° Lat/Lon grid was calculated from a 70 x 70 m digital elevation model. Since N deposition increases with precipitation the coarse scale deposition were scaled with the finer scale precipitation data so that areas with lower precipitation in a coarse scale cell receive less deposition and vice versa. The mean deposition of all smaller scale cells remain the same as the respective coarse scale values. Additionally, we took into account altitudinal effects because of the high variation of altitude within the coarse scale grid cells. Above 1000 m a.s.l. N ion concentrations in wet deposition increase by 2.5% per 100 altitudinal meters whereas below 1000 m concentrations are independent from altitude (Umweltbundesamt, 1998). These rules were used to downscale wet N deposition whereas dry deposition was taken from the coarse scale grids as they were. We used three different N deposition scenarios for the years 2010, 2030 and 2050. The current legislation (CLE) scenario with revised Gothenburg Protocol emissions until 2030, the technically maximum feasible emission reduction scenario (MFR) until 2030 (both no further reduction between 2030 and 2050), and the 2010 deposition values as baseline with no further reduction (B10).

2.9. Classifying alliances into the EUNIS classes

Critical loads are defined for habitat types of the European Nature Information System (EUNIS, http://eunis.eea.europa.eu/), but not for alliances of the syntaxonomical system. Moreover, the available 100 x 100 m habitat map of Austria also uses the EUNIS classification system (Dirnböck & Peterseil, 2013). We hence assigned the 66 alliances to a total of 43 EUNIS categories. Thereby, some alliances could be classified into several different categories, since habitat types in EUNIS are more broadly defined (see Appendix, Tab.1). In such cases, an alliance was assigned the average CL of all the respective EUNIS categories. By contrast, some EUNIS categories included more than one alliance – with all of them receiving the same CL in these cases (Appendix, Tab.1)

2.10. Risk maps

Based on the different N deposition and climate change scenarios we finally computed risk maps separately for temperature, drought and nitrogen deposition as well as for the combination of these three factors. Risk was thereby defined as the magnitude of exceedance of the empirical critical load for nitrogen, taken from Bobbink & Hettelingh, (2010), or critical climatic thresholds, respectively. For each 100 x 100 m cell, exceedance was calculated as the distance between the current, or predicted future, mean annual temperature, annual precipitation sum, or nitrogen deposition and the critical climatic thresholds of the local habitat type (Fig. 1) or its critical load of nitrogen, respectively. As we assumed that the sensitivity of a community is proportional to its niche width, i.e. that 'generalists' are more tolerant to exceedance of critical threshold than 'specialists', we further divided the calculated distance by the respective niche width, i.e. the maximum breadth of the habitat type's niche along the temperature and precipitation axes of Fig. 1 for temperature and water limitation, respectively; or by the critical load in case of nitrogen deposition.

By scaling the calculated exceedance values to [0,1], i.e. dividing them by the respective maximum values, all exceedance values were re-aligned on a relative scale and effects of different measurement scales of temperature (°C), precipitation (mm) and N deposition (kg N / ha / y) were removed. The final maps presented here hence allow to identify areas of highest relative risk in a region, but not to quantify absolute risk. Information on the latter can, however, be extracted from the exceedance maps that underly these relative risk maps if desired.

These scaled values were then combined into joint risk measure by means of the Euclidean distance metric. To keep this risk measures conservative, we computed all risk maps by assuming that the EUNIS-habitat type present in a certain raster cell according to the habitat map is locally represented by the syntaxonomical alliance with the lowest risk value (in all cases where more than one of the 66 alliances was assigned to respective EUNIS category).

2.11. *Risk differences among scenarios, habitat types and regions*

We evaluated differences in average risk to Austrian habitat types among climatic and N scenarios using a random sample of 15% of all 100 x 100 m cells (n = 819980). Statistical significance was assessed by means of a Kruskal Wallis test using Dunn's Test of multiple Comparison as a post-hoc test. The same approach was applied to compare differences in risk among ten EUNIS categories, with number of samples >20.

In order to pinpoint conservation implications of the combined climate and nitrogen deposition scenarios we additionally overlaid the maps of calculated single-factor- and total risk, as well as a map of the 80% quantile of combined risk values, with a map of the Natura2000 network in Austria (http://www.eea.europa.eu/).

3. **Results**

3.1. Risk maps

The full factorial combination of three N-deposition scenarios, two climate change scenarios and two time horizons (2030 and 2050) yielded a total of 12 different future risk maps for Austria (see Fig.3 as an example).

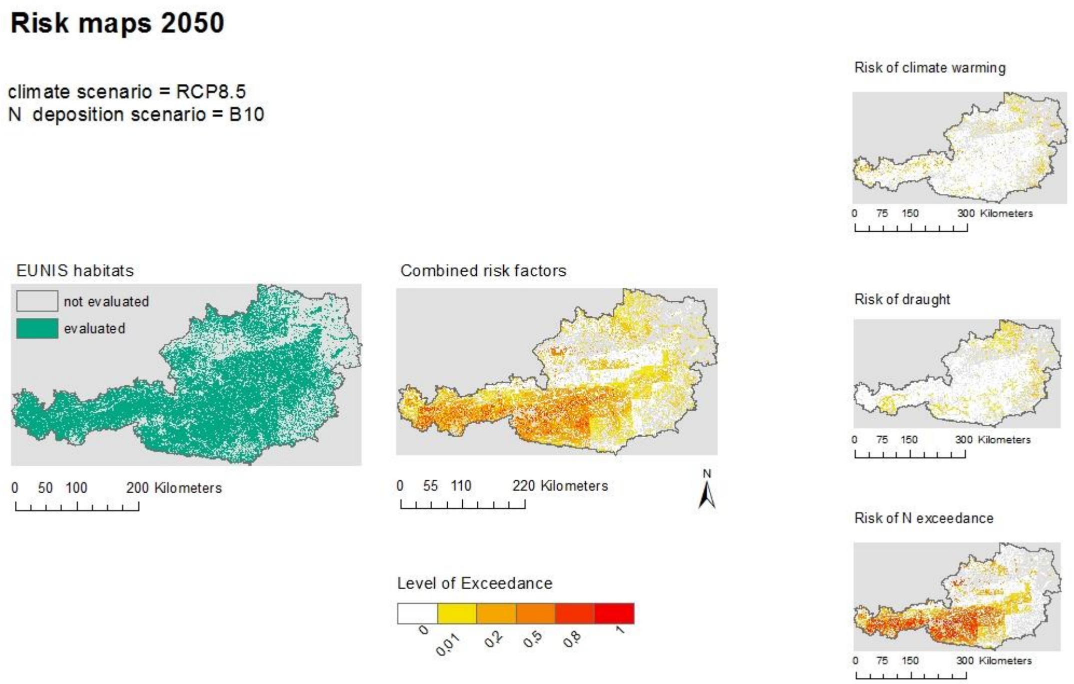

Fig.3 Risk maps of a 2050 scenario combining RCP8.5 and B10. Risk levels are standardized to [0,1] with 0 indicating no risk and 1 maximum risk. Areas where none of the modelled habitat types occur (grey) have not been evaluated (further maps in Appendix: Fig.1).

Calculated total risk values are dominated by N-risk at each time step, with mean values approximately an order of magnitude larger as those of climatic risk values (Fig. 3). This ‘pattern’ holds even when combining the most pronounced climatic scenario with the most modest N-deposition scenario. With respect to N-risk, our evaluation demonstrates a significant decline under both CLE and MFR as compared to B10 (Fig.4b). Thus, if combined risk is averaged across all scenarios for each point in time, overall combined risk is declining (Fig.4a). Fig4.c depicts increasing combined risk value in the RCP8.5 scenario, as opposed to the RCP2.6 scenario. Kruskal Wallis tests show that differences in risks between climate and deposition scenarios and between time steps are significant ($p<0.001$, Appendix: Tab.4). Post-hoc Dunn test pairwise comparisons are all significant ($p<0.001$, Appendix: Tab.5), except for the N-risk between 2030 and 2050 (Appendix, Tab.3).

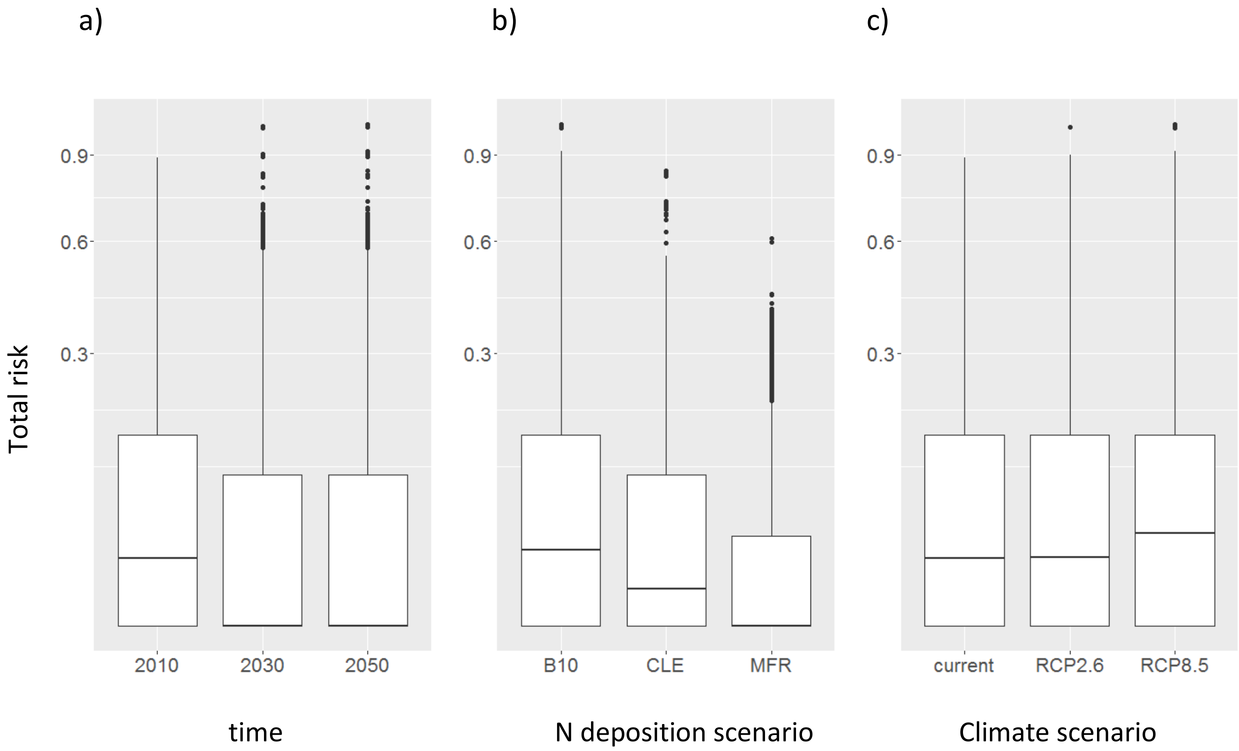

Fig.4 Differences in combined risk values between a) time steps, b) N deposition scenarios and c) climate scenarios. Category '2010' and 'current' represent combinations of B10 and current climatic conditions. In c) B10 is retained as the deposition scenario, whereas for the other categories in a) values represent averages over all considered N deposition and climatic scenarios and b) averages over the two climatic scenarios.

3.2. Risks within special protection sites

Depending on the combination of climate, deposition scenarios and time step, 23-40% of the Austrian Natura 2000 area is affected by combined risk, i.e. at least one factor exceeds the respective critical threshold. In total, 6-7% of the Natura 2000 area are hot spots i.e. exposed to the highest 20% of risk values (= 80th quantile of total risk values). In comparison 34-62% of the non-protected area experiences combined risk, with 6-12% as hot spots. Lowest risk values in- and outside special protection sites are found when RCP2.6 and MFR scenarios are combined, highest risk values under a combination of RCP8.5 and B10. In general, the proportion of area affected by combined risk depends on the particular combination of scenarios applied, but on average over all scenarios and all the area combined risk increases until 2050 (Fig. 6).

Not only underpins the magnitude of risk that N deposition is the dominant risk factor, but also the percentage area affected: 13-28% of Natura2000 areas are on risk of eutrophication, but only 2-12% are on risk from too high temperature or too low precipitation (Appendix, Tab.10).

A map of the hot spots according to the scenario with the highest total risk in 2050 (RCP8.5, B10), demonstrates that combined risk is especially pronounced in the southern regions of the Austrian Alps (Fig. 7). Again, this pattern of combined risk largely reflects the distribution of N-risk (compare Fig.3 N).

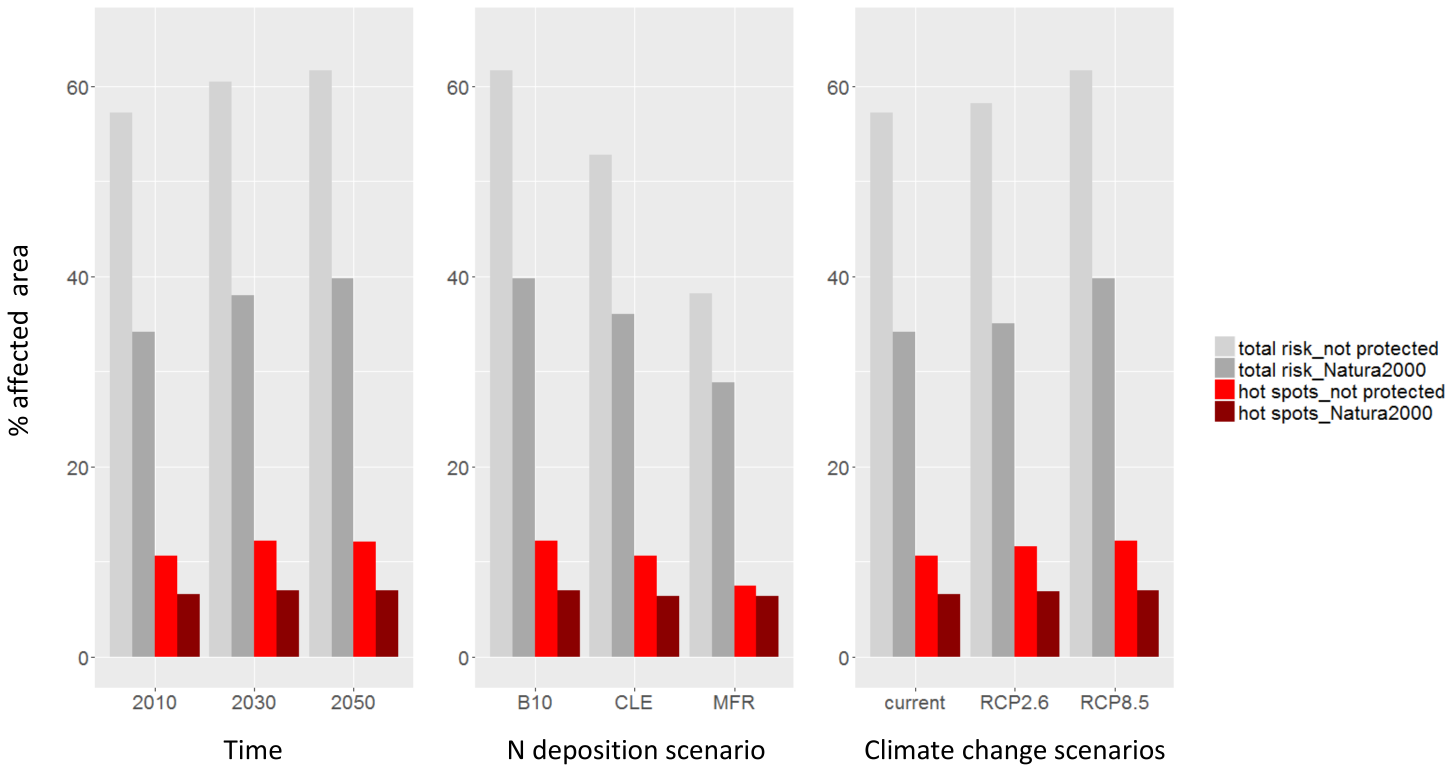

Fig.6 Area affected by combined risk (total risk > 0) and percentage of hot spots (80th quantile of total risk > 0) over time, and in different N deposition and climate change scenarios within Natura2000 sites and non-protected area.

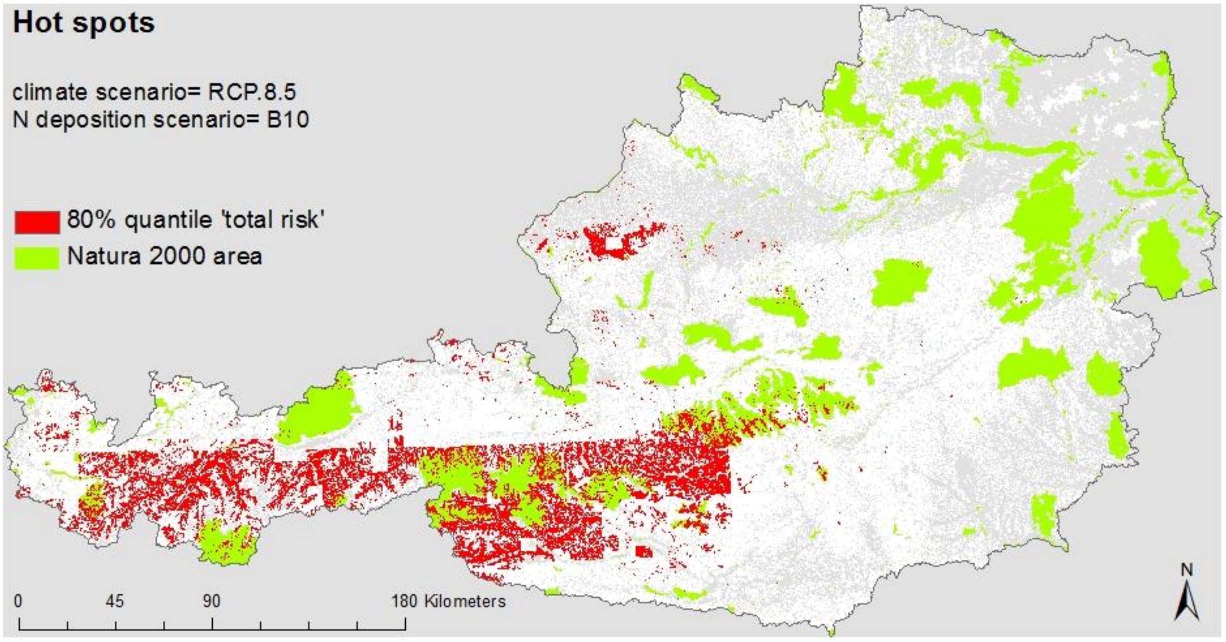

Fig.7 Location of Natura 2000 sites (as of 2015) and areas that are at high risk (top 20% of values >0) in the scenario combination with the highest combined risk (RCP8.5, B10).

3.3. Habitats at risk

Across all scenarios, up to 27% of 'Coniferous Woodland' [G3] is affected by combined risk and in sum experiences the highest total risk values. The maximum combined risk value was found in the sub-group of 'Boreal Bog Conifer Woodland' [G3.D]. Among single risk factors, N-risk is also highest for 'Coniferous Woodland' [G3]. 'Central Alpine Arid Grassland' [E1.24] face maximum drought risk and maximum risk of temperature increase is highest in 'Arid Subcontinental Steppic Grassland' [E1.22] (under RCP8.5) or 'Acid Alpine and Subalpine Grassland' [E4.3] (under RCP2.6).

In Fig. 8, yet again, dominance in risk of N exceedance is prominent. Especially bogs, mires, alpine habitats and coniferous woodland are exposed to N-risk, though mires and alpine grassland are also affected by warming-risk. Habitats of dry grassland show particular risk from drought and warming. Medians in single and combined risks are significantly different between habitats ($p<0.001$, Appendix: Tab.6-9).

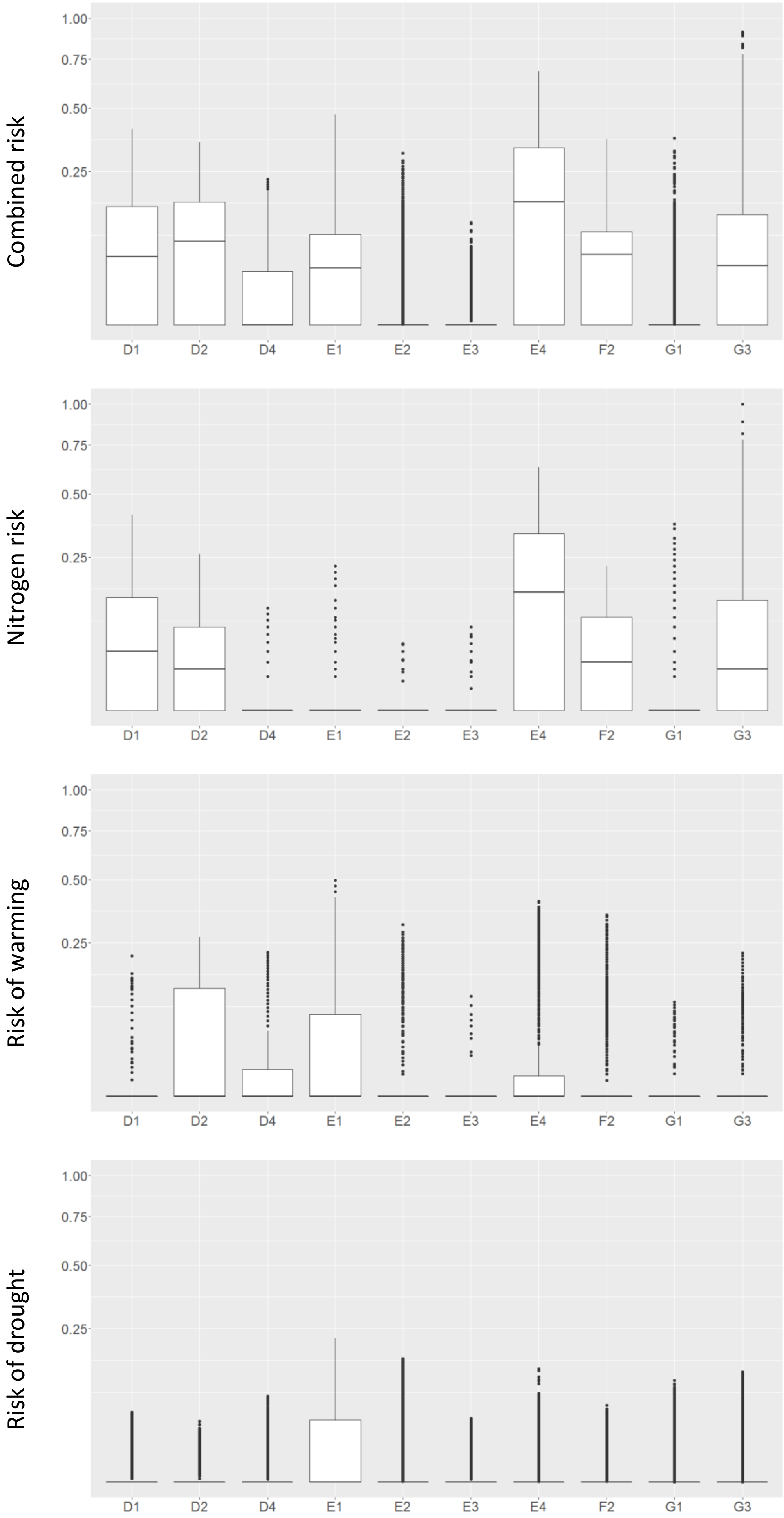

Fig.8 Risks of single factor and 'combined risk' regarding 10 EUNIS level 2 categorized habitats of all evaluated area

D1 = Raised and blanket bogs

D2 = Valley mires, poor fens and transition mires

D4 = Base-rich fens and calcareous spring mires

E1 = Dry grassland

E2 = Mesic grassland

E3 = Seasonally wet and wet grassland

E4 = Alpine and subalpine grassland

F2 = Arctic, alpine and subalpine scrub

G1 = Broadleaved decidious woodland

G3 = Coniferous woodland

4. Discussion

This study provides us with a new method to identify areas and habitats that are of special concern if interactive effects of climate change and nitrogen deposition are to be considered in conservation strategies. Our method combines current state of the art assessment tools in climate change and N deposition impact studies into a common framework. Its application to Austria demonstrates that abundant habitats such as coniferous woodlands are and will experience high risk of combined impacts due to their distribution in areas with high N deposition, the general higher N deposition in these habitats and their high climate risk. Also very oligotrophic habitats (e.g. bogs) with low critical loads are facing high combined risk. Taking proportion of area affected, average risk and high risk together, alpine habitats in the southern part of the Central Alps are disproportionally at risk.

Our method gave us new insights into the magnitude and the distribution of combined risks from N deposition and climate change in Austria. As special protection sites are an implemented conservation strategy in Europe, we were interested in the proportion of areas at risk following our evaluation method. A concerning outcome is that, regardless of the scenario, a constant of 6-7% of the Natura 2000 area is exposed to the highest risk values (top 20% of all values). Most of the area is found in the southern Austrian alpine region, where high N deposition prevails from high N emission in the Italian Po valley (Rogora et al., 2006). A recent meta-analysis by Humbert et al. (2016) showed that species richness in mountain grassland is negatively and additively influenced by increasing dose and duration of N deposition. Hence Austrian alpine and subalpine grassland habitats should be prioritized in research about interactive effects and respective conservation efforts. The same can be said, and was highlighted with our method, for habitats particularly vulnerable to both climate change (Essl et al., 2012) and N deposition (Bobbink et al., 2010; Bobbink et al., 1998) such as oligotrophic bogs.

There are, however, limitations to our approach. Most importantly, the calculated metric is not scaled well to the potential ecological or biological impact that the risks might exert. Put it another way, it is well possible that an area with a small risk of warming or drought has an equally large or even larger impact on plant communities than a much larger N-risk value. Our results that airborne N deposition may exert a more intense pressure on Austrian plant communities than climate warming over the next decades may not be true in general. As an example, due to the wide distribution of coniferous forests in areas with high N deposition input, our evaluation resulted in high levels of combined risk. Since Austrian Norway spruce forests are exposed to high N deposition (Jandl et al., 2012; Jost et al., 2011) and are particularly vulnerable to climate change(Lexer et al., 2002; Seidl et al., 2011), we deem this an equitable result . However, interactions could even lower the magnitude of total effects because warming induced tree growth might lower soil N availability (McDonnell et al., 2014). Also the very dry sites showing disproportionate total risk 'Arid Subcontinental Steppic Grassland' [E1.22] and 'Central Alpine Arid Grassland' [E1.24]) might not be sensitive to N deposition as shown in Simkin et al. (2016). They might also react quite different to climate change. Baatar et al. (2016, unpubl.) suggests dry grassland habitats of higher elevation are at risk of losing area due to upward expansion of more warm adapted similar habitat types, which is not the case for lowland grasslands.

The logical advance in our method would be to include N deposition effects directly into the empirical niche functions. This is currently in development for large parts of Europe but still hampered in many other parts of the world by the limited availability of on-ground measurements to calibrate N-driven niche functions for a large enough number of species (Reinds et al., 2014; Rowe et al., 2015). Also, more climate variables could be implemented to achieve a finer representation of climate constraints. The results of our method particularly depend upon the quality of the habitat map. In some EUNIS habitats the risk values relied on single alliances (e.g. some grassland types) whereas for others they relied on many (e.g. deciduous forests). Hence availability of high resolution habitat maps is key to an unbiased assessment. Considerable progress has been made in some parts of Europe in providing such maps (Kuttner et al., 2015).

Conclusion

Empirical studies and dynamic models evaluate in detail interactive effects of N deposition and climate change at specific sites and given conditions. Since our method is based on standard procedures, it is well possible to be applied to large areas, with further data input deemed improvable. Albeit interactive effects are not always considered negative for given habitat, we propose this method to be a simple tool for broad scale risk assessment that might help to prioritize and guide conservation strategies.

5. References

Assessment, M.E., 2005. Ecosystem and human well-being: biodiversity synthesis. World Resour. Inst. Wash. DC.

Baatar, U.-O., Dirnböck, T., Essl, F., Moser, D., Wessely, J., Willner, W., Dullinger, S., 2016. Climate effects on habitat types in Austria. unpubl.

Bellard, C., Bertelsmeier, C., Leadley, P., Thuiller, W., & Courchamp, F. (2012). Impacts of climate change on the future of biodiversity. Ecology Letters, 15(4), 365–377.

Bobbink, R., & Hettelingh, J.-P. (2010). Review and revision of empirical critical loads and dose-response relationships. In Proceedings of an expert workshop, Noordwijkerhout (Vol. 2325).

Bobbink, R., Hicks, K., Galloway, J., Spranger, T., Alkemade, R., Ashmore, M., Bustamante, M., Cinderby, S., Davidson, E., Dentener, F., Emmett, B., Erisman, J.W., Fenn, M., Gilliam, F., Nordin, A., Pardo, L., De Vries, W., 2010. Global assessment of nitrogen deposition effects on terrestrial plant diversity: a synthesis. Ecol Appl 20, 30–59.

Bobbink, R., Hornung, M., Roelofs, J.G., 1998. The effects of air-borne nitrogen pollutants on species diversity in natural and semi-natural European vegetation. J. Ecol. 86, 717–738.

Butler, S. M., Melillo, J. M., Johnson, J. E., Mohan, J., Steudler, P. A., Lux, H., … Bowles, F. (2012). Soil warming alters nitrogen cycling in a New England forest: implications for ecosystem function and structure. Oecologia, 168(3), 819–828.

Chytrý, M., Hennekens, S.M., Jiménez-Alfaro, B., Knollová, I., Dengler, J., Jansen, F., Landucci, F., Schaminée, J.H.J., Aćić, S., Agrillo, E., Ambarlı, D., Angelini, P., Apostolova, I., Attorre, F., Berg, C., Bergmeier, E., Biurrun, I., Botta-Dukát, Z., Brisse, H., Campos, J.A., Carlón, L., Čarni, A., Casella, L., Csiky, J., Ćušterevska, R., Dajić Stevanović, Z., Danihelka, J., De Bie, E., Ruffray, P., De Sanctis, M., Dickoré, W.B., Dimopoulos, P., Dubyna, D., Dziuba, T., Ejrnæs, R., Ermakov, N., Ewald, J., Fanelli, G., Fernández-González, F., Fitzpatrick, Ú., Font, X., García-Mijangos, I., Gavilán, R.G., Golub, V., Guarino, R., Haveman, R., Indreica, A., Işık Gürsoy, D., Jandt, U., Janssen, J.A.M., Jiroušek, M., Kącki, Z., Kavgacı, A., Kleikamp, M., Kolomiychuk, V., Krstivojević Ćuk, M., Krstonošić, D., Kuzemko, A., Lenoir, J., Lysenko, T., Marcenò, C., Martynenko, V., Michalcová, D., Moeslund, J.E., Onyshchenko, V., Pedashenko, H., Pérez-Haase, A., Peterka, T., Prokhorov, V., Rašomavičius, V., Rodríguez-Rojo, M.P., Rodwell, J.S., Rogova, T., Ruprecht, E., Rūsiņa, S., Seidler, G., Šibík, J., Šilc, U., Škvorc, Ž., Sopotlieva, D., Stančić, Z., Svenning, J., Swacha, G., Tsiripidis, I., Turtureanu, P.D., Uğurlu, E., Uogintas, D., Valachovič, M., Vashenyak, Y., Vassilev, K., Venanzoni, R., Virtanen, R., Weekes, L., Willner, W., Wohlgemuth, T., Yamalov, S., 2016. European Vegetation Archive (EVA): an integrated database of European vegetation plots. Appl. Veg. Sci. 2016 Vol191 Pp173-180 173.

De Marco, A., Proietti, C., Cionni, I., Fischer, R., Screpanti, A., & Vitale, M. (2014). Future impacts of nitrogen deposition and climate change scenarios on forest crown defoliation. Environmental Pollution, 194, 171–180.

de Vries, W., Posch, M., 2011. Modelling the impact of nitrogen deposition, climate change and nutrient limitations on tree carbon sequestration in Europe for the period 1900–2050. Environ. Pollut. 2011 Vol15910 Pp2289-2299 2289.

Dillon, M. E., Wang, G., & Huey, R. B. (2010). Global metabolic impacts of recent climate warming. Nature, 467(7316), 704–6.
Dirnböck, T., Grandin, U., Bernhardt-Römermann, M., Beudert, B., Canullo, R., Forsius, M., … Uzięblo, A. K. (2014). Forest floor vegetation response to nitrogen deposition in Europe. Global Change Biology, 20(2), 429–440.
Dirnböck, T., Peterseil, J., 2013. UNECE ICP Modelling & Mapping Datenanfrage 2013-2014 1.Zwischenbericht. Umweltbundesamt GmbH.
Dullinger, S., Gattringer, A., Thuiller, W., Moser, D., Zimmermann, N. E., Guisan, A., … Hülber, K. (2012). Extinction debt of high-mountain plants under twenty-first-century climate change. Nature Climate Change, 2(8), 619–622.
Essl, F., Dullinger, S., Moser, D., Rabitsch, W., & Kleinbauer, I. (2012). Vulnerability of mires under climate change: implications for nature conservation and climate change adaptation. Biodiversity and Conservation, 21(3), 655–669.
Galloway, J. N., Dentener, F. J., Capone, D. G., Boyer, E. W., Howarth, R. W., Seitzinger, S. P., … Vorosmarty, C. J. (2004). Nitrogen cycles: past, present, and future. Biogeochemistry, 70(2), 153–226.
Grabherr, G., & Mucina, L. (1993). Natürliche waldfreie Vegetation Die Pflanzengesellschaften Österreichs. Jena [u.a.]: G. Fischer.
Guisan, A., & Rahbek, C. (2011). SESAM - a new framework integrating macroecological and species distribution models for predicting spatio-temporal patterns of species assemblages. Journal of Biogeography, 38(8), 1433–1444.
Guntiñas, M. E., Leirós, M. C., Trasar-Cepeda, C., & Gil-Sotres, F. (2012). Effects of moisture and temperature on net soil nitrogen mineralization: A laboratory study. European Journal of Soil Biology, 48, 73–80.
Humbert, J.-Y., Dwyer, J. M., Andrey, A., & Arlettaz, R. (2016). Impacts of nitrogen addition on plant biodiversity in mountain grasslands depend on dose, application duration and climate: a systematic review. Global Change Biology, 22(1), 110–120.
Isotta, F. A., Frei, C., Weilguni, V., Perčec Tadić, M., Lassègues, P., Rudolf, B., … Vertačnik, G. (2014). The climate of daily precipitation in the Alps: development and analysis of a high-resolution grid dataset from pan-Alpine rain-gauge data: CLIMATE OF DAILY PRECIPITATION IN THE ALPS. International Journal of Climatology, 34(5), 1657–1675.
Jandl, R., Smidt, S., Mutsch, F., Fürst, A., Zechmeister, H., Bauer, H., & Dirnböck, T. (2012). Acidification and Nitrogen Eutrophication of Austrian Forest Soils. Applied and Environmental Soil Science, 2012, 1–9.
Jost, G., Dirnböck, T., Grabner, M.-T., & Mirtl, M. (2011). Nitrogen Leaching of Two Forest Ecosystems in a Karst Watershed. Water, Air, & Soil Pollution, 218(1–4), 633–649.
Kuttner, M., Essl, F., Peterseil, J., Dullinger, S., Rabitsch, W., Schindler, S., Hubler, K., Gattringer, A., Moser, D., 2015. A new high-resolution habitat distribution map for Austria, Liechtenstein, southern Germany, South Tyrol and Switzerland. J. Prot. Mt. Areas Res. Volume 7.
Lexer, M.J., Hönninger, K., Scheifinger, H., Matulla, C., Groll, N., Kromp-Kolb, H., Schadauer, K., Starlinger, F., Englisch, M., 2002. The sensitivity of Austrian forests to scenarios of climatic change: a large-scale risk assessment based on a modified gap model and forest inventory data. For. Ecol. Manag. 162, 53–72.
McClean, C. J., van den Berg, L. J. L., Ashmore, M. R., & Preston, C. D. (2011). Atmospheric nitrogen deposition explains patterns of plant species loss. Global Change Biology, 17(9), 2882–2892.

McDonnell, T. C., Belyazid, S., Sullivan, T. J., Sverdrup, H., Bowman, W. D., & Porter, E. M. (2014). Modeled subalpine plant community response to climate change and atmospheric nitrogen deposition in Rocky Mountain National Park, USA. Environmental Pollution, 187, 55–64.

Moss, R. H., Edmonds, J. A., Hibbard, K. A., Manning, M. R., Rose, S. K., van Vuuren, D. P., … Wilbanks, T. J. (2010). The next generation of scenarios for climate change research and assessment. Nature, 463(7282), 747–756.

Pardo, L.H., Fenn, M.E., Goodale, C.L., Geiser, L.H., Driscoll, C.T., Allen, E.B., Baron, J.S., Bobbink, R., Bowman, W.D., Clark, C.M., others, 2011. Effects of nitrogen deposition and empirical nitrogen critical loads for ecoregions of the United States. Ecol. Appl. 21, 3049–3082.

Parmesan, C. (2006). Ecological and evolutionary responses to recent climate change. Annual Review of Ecology Evolution and Systematics, 37, 637–669.

Pereira, H. M., Leadley, P. W., Proenca, V., Alkemade, R., Scharlemann, J. P., Fernandez-Manjarres, J. F., … Walpole, M. (2010). Scenarios for global biodiversity in the 21st century. Science, 330(6010), 1496–501.

Porter, E. M., Bowman, W. D., Clark, C. M., Compton, J. E., Pardo, L. H., & Soong, J. L. (2012). Interactive effects of anthropogenic nitrogen enrichment and climate change on terrestrial and aquatic biodiversity. Biogeochemistry, 114(1), 93–120.

Posch, M., Hettelingh, J. P., & De Smet, P. A. M. (2001). Characterization of critical load exceedances in Europe. Water Air and Soil Pollution, 130(1–4), 1139–1144.

Reinds, G. J., & Mol-Dijkstra, J. P. (2014). VSD+ PROPS: Recent Developments. In J. Slootweg, M. Posch, J. P. Hettelingh, & E. A. M. Mathijssen-Spiekman, Modelling and Mapping the impacts of atmospheric deposition on plant species diversity in Europe (pp. 47–53). Bilthoven: Rijksinstituut voor Volksgezondheid en Milieu RIVM.

Rodwell, J., Dring, J., Hoda, P., Mersinllari, M., Mullaj, A., Pignatti, S., & others. (2002). Plant communities of Albania-A preliminary overview. Annali Di Botanica, 2.

Rogora, M., Mosello, R., Arisci, S., Brizzio, M. C., Barbieri, A., Balestrini, R., … Probst, A. (2006). An Overview of Atmospheric Deposition Chemistry over the Alps: Present Status and Long-term Trends. Hydrobiologia, 562(1), 17–40.

Rowe, E.C., Wamelink, G.W., Smart, S.M., Butler, A., Henrys, P.A., Van Dobben, H., Reinds, G.J., Evans, C.D., Kros, J., 2015. Field survey based models for exploring nitrogen and acidity effects on plant species diversity and assessing long-term critical loads, in: Critical Loads and Dynamic Risk Assessments: Nitrogen, Acidity and Metals in Terrestrial and Aquatic Ecosystems. Springer, Dordrecht [u.a.], pp. 297–326.

Sala, O.E., Chapin, F.S., 3rd, Armesto, J.J., Berlow, E., Bloomfield, J., Dirzo, R., Huber-Sanwald, E., Huenneke, L.F., Jackson, R.B., Kinzig, A., Leemans, R., Lodge, D.M., Mooney, H.A., Oesterheld, M., Poff, N.L., Sykes, M.T., Walker, B.H., Walker, M., Wall, D.H., 2000. Global biodiversity scenarios for the year 2100. Science 287, 1770–4.

Seidl, R., Rammer, W., & Lexer, M. J. (2011). Climate change vulnerability of sustainable forest management in the Eastern Alps. Climatic Change, 106(2), 225–254.

Simkin, S. M., Allen, E. B., Bowman, W. D., Clark, C. M., Belnap, J., Brooks, M. L., … others. (2016). A continental analysis of ecosystem vulnerability to atmospheric nitrogen deposition.

Simpson, D., Benedictow, A., Berge, H., Bergström, R., Emberson, L. D., Fagerli, H., … Wind, P. (2012). The EMEP MSC-W chemical transport model – technical description. Atmospheric Chemistry and Physics, 12(16), 7825–7865.

Stevens, C. J., Dupre, C., Dorland, E., Gaudnik, C., Gowing, D. J., Bleeker, A., … Dise, N. B. (2010). Nitrogen deposition threatens species richness of grasslands across Europe. Environ Pollut, 158(9), 2940–5.
Thuiller, W., Damien, G., Engler, R., Breiner, F., 2012. Package "biomod2."
Umweltbundesamt, 1998. Kartierung der nassen Deposition in Österreich, UBA-BE 104. Umweltbundesamt GmbH, Wien.
Willner, W., & Grabherr, G. (2007). Textband Die Wälder und Gebüsche Österreichs ein Bestimmungswerk mit Tabellen (1. Aufl.). München: Elsevier, Spektrum Akad. Verl.
Willner, W., Tichỳ, L., Chytrỳ, M., 2009. Effects of different fidelity measures and contexts on the determination of diagnostic species. J. Veg. Sci. 20, 130–137.
Zavaleta, E. S., Shaw, M. R., Chiariello, N. R., Mooney, H. A., & Field, C. B. (2003). Additive effects of simulated climate changes, elevated CO2, and nitrogen deposition on grassland diversity. Proceedings of the National Academy of Sciences, 100(13), 7650–7654.
Zimmermann, N.E., Yoccoz, N.G., Edwards, T.C., Meier, E.S., Thuiller, W., Guisan, A., Schmatz, D.R., Pearman, P.B., 2009. Climatic extremes improve predictions of spatial patterns of tree species. Proc. Natl. Acad. Sci. 106, 19723–19728.

6. **Appendix**

Tab.1 Alliances as defined in Grabherr et al. (1994), Grabherr & Mucina (1994) und Willner et al. (2007), their alignment with the EUNIS classification and the respective critical loads.

ALLIANCE	EUNIS_CODE	CL N	CLN DERIVED FROM	EUNIS LEVEL 2 NAMES
ABIETI-PICEION	G3.1 G3	10	G3.1	Coniferous woodland
AGROSTION SCHRADERIANAE	E4 E4.3	5	E4.3	Alpine and subalpine grasslands
ALCHEMILLO-POION SUPINAE	E2 E2.1	NA	E2.1	Mesic grasslands
ALNION GLUTINOSAE	G1 G1.2	NA	G1.2	Broadleaved deciduous woodland
ALNION INCANAE	G1 G1.A	NA	G1.A	Broadleaved deciduous woodland
ALNION VIRIDIS	F2 F2.3	15	F2.3	Dry heaths
ALYSSO ALYSSOIDIS-SEDION ALBI	E1 E1.1	15	E1.1	Dry grasslands
ALYSSO SAXATILIS-FESTUCION PALLENTIS	E1 E1.1	15	E1.1	Dry grasslands
ARABIDOPSIDION THALIANAE	E1 E1.1	15	E1.1	Dry grasslands
ARRHENATHERION	E2 E2.2	20	E2.2	Mesic grasslands
BETULION PUBESCENTIS	G1 G1.5	NA	G1.5	Broadleaved deciduous woodland
BROMION ERECTI	E1 E1.2	15	E1.2	Dry grasslands
BROMO PANNONICI-FESTUCION PALLENTIS	E1 E1.1	15	E1.1	Dry grasslands
CALAMAGROSTION VARIAE	E4	5	E4	Alpine and subalpine grasslands
CALTHION	E3 E3.4	NA	E3.4	Seasonally wet and wet grasslands
CARICION ATROFUSCO-SAXATILIS	D4 D4.2 D4.1	15	D4.1 = D4.2	Base-rich fens and calcareous spring mires
CARICION AUSTROALPINAE	E4	5	E4	Alpine and subalpine grasslands
CARICION CURVULAE	E4 E4.3	5	E4.3	Alpine and subalpine grasslands
CARICION DAVALLIANAE	D4.1 D4 D4.2	15	D4.1 = D4.2	Base-rich fens and calcareous spring mires
CARICION FERRUGINAE	E4	5	E4	Alpine and subalpine grasslands
CARICION FIRMAE	E4	5	E4	Alpine and subalpine grasslands
CARICION FUSCAE	D2	10	D2	Valley mires, poor fens and transition mires
CARICION LASIOCARPAE	D2 D2.3	10	D2.3	Valley mires, poor fens and transition mires
CARPINION BETULI	G1 G1.A	15	G1.A	Broadleaved deciduous woodland
CIRSIO-BRACHYPODION PINNATI	E1 E1.2	15	E1.2	Dry grasslands

ALLIANCE	EUNIS_CODE	CL N	CLN DERIVED FROM	EUNIS LEVEL 2 NAMES
CNIDION	E3 E3.4	NA	E3.4	Seasonally wet and wet grasslands
CORYNEOPHORION CANESCENTIS	E1 E1.9	15	E1.9	Dry grasslands
CYNOSURION	E2 E2.2 E2.1 E2.6	20	E2.2	Mesic grasslands
DESCHAMPSION	E3 E3.5 E3.4	15	E3.4	Seasonally wet and wet grasslands
DIANTHO LUMNITZERI-SESLERION	E1 E1.2 E1.1	15	E1.1 = E1.2	Dry grasslands
ERICION CARNEAE	F2 F2.2	10	F2.2	Arctic, alpine and subalpine scrub
ERICO-PINION SYLVESTRIS	G3 G3.E G3.4	5	G3.E = G3.4	Coniferous woodland
FAGION SYLVATICAE	G1 G1.6 G3 G3.1	10	G1.6 = G3.1	Broadleaved deciduous woodland & Coniferous woodland
FESTUCION VAGINATAE	E1 E1.1	15	E1.1	Dry grasslands
FESTUCION VALESIACAE	E1 E1.22	15	E1.22	Dry grasslands
FESTUCION VARIAE	E4 E4.3	5	E4.3	Alpine and subalpine grasslands
FRAXINO ORNI-OSTRYION	G1 G1.7	10	G1.7	Broadleaved deciduous woodland
GENISTION PILOSAE	F4.2	10	F4.2	Dry heaths
HYPERICO PERFORATI-SCLERANTHION PERENNIS	E1 E1.1 E1.9	15	E1.1	Dry grasslands
JUNCION TRIFIDI	E4 E4.3	5	E4.3	Alpine and subalpine grasslands
LOISELEURIO-VACCINION	F2 F2.2	10	F2.2	Arctic, alpine and subalpine scrub
MOLINION	E2 E2.1 E2.2 E3 E3.4 E3.5	17.5	mean E2.2 & E3.5	Mesic grasslands & Seasonally wet and wet grasslands
NARDION STRICTAE	E4 E4.3	5	E4.3	Alpine and subalpine grasslands
NARDO-AGROSTION TENUIS	**E4** E4.3	**5**	**E4.3**	**Alpine and subalpine grasslands**
NARDO-JUNCION SQUARROSI	E3 E3.5	15	E3.5	Seasonally wet and wet grasslands

ALLIANCE	EUNIS_CODE	CL N	CLN DERIVED FROM	EUNIS LEVEL 2 NAMES
ONONIDO ROTUNDFOLII-PINION SYLVESTRIS	G3 G3.4	5	G3.4	Coniferous woodland
OXYOCOCCO-EMPETRION HERMAPHRODITI	D1 D1.1	5	D1.1	Raised and blanket bogs
OXYTROPIDO-ELYNION	E4	5	E4	Alpine and subalpine grasslands
PHYTEUMO-TRISETION	E2 E2.3	20	E2.3	Mesic grasslands
PINION MUGI	F2 F2.4	15	F2.4	Arctic, alpine and subalpine scrub
POION ALPINAE	E4 E4.5	NA	E4.5	Alpine and subalpine grasslands
POLYGONO-TRISETION	E2 E2.3	20	E2.3	Mesic grasslands
QUERCION PUBESCENTI-PETRAE	G1 G1.7	10	G1.7	Broadleaved deciduous woodland
QUERCION ROBORIS	G1 G1.8	10	G1.8	Broadleaved deciduous woodland
RHODODENDRO-VACCINION	F2 F2.2	10	F2.2	Arctic, alpine and subalpine scrub
RHYNCHOSPORION ALBAE	D2 D2.3 D1 D1.1 D1.2	7.5	mean D2.3 & D1.1 (= D1.2)	Raised and blanket bogs & Transition mires and quaking bogs
SALICION AURITAE	G1 G1.2	NA	G1.2	Broadleaved deciduous woodland
SALICION CINERAE	G1 G1.2	NA	G1.2	Broadleaved deciduous woodland
SEDO-SCLERANTHION BIENNIS	E1 E1.1	15	E1.1	Dry grasslands
SESLERION COERULEAE	E4	5	E4	Alpine and subalpine grasslands
SPHAGNION MEDII	D1 D1.1	5	D1.1	Raised and blanket bogs
STIPO-POION XEROPHILAE	E1 E1.24	15	E1.24	Dry grasslands
THERO-AIRION	E1 E1.1	15	E1.1	Dry grasslands
TILIO-ACERION	G1 G1.A	15	G1.A	Broadleaved deciduous woodland
VACCINIO ULIGINOSI-PINION SYLVESTRIS	G3 G3.D G3.E	5	G3.D = G3.E	Coniferous woodland
VIOLION CANINAE	E1 E1.7	10	E1.7	Dry grasslands

Tab.2 Ensemble models evaluation with ROC. EM_ROC= ensemble model evaluation for each species, meanROC = mean ROC of an alliance. Names of syntaxa and characteristic species follow Grabherr et al. (1994), Grabherr & Mucina (1994) und Willner et al. (2007). Species not listed have not been represented with sufficient frequency in the relevé dataset.

Alliance	Species	EM_ROC	meanROC
Abieti-Piceion	*Galium rotundifolium*	0.796	0.795
	Orthilia secunda	0.794	
Agrostion schraderianae	*Agrostis schraderiana*	0.929	0.97
	Alchemilla alpina	0.974	
	Carex aterrima	0.984	
	Festuca picturata	0.988	
	Gnaphalium norvegicum	0.968	
	Pedicularis recutita	0.975	
Alchemillo-Poion supinae	*Alchemilla xanthochlora*	0.832	0.892
	Poa supina	0.952	
Alnion glutinosae	*Alnus glutinosa*	0.737	0.832
	Carex elongata	0.852	
	Dryopteris cristata	0.877	
	Ribes nigrum	0.871	
	Scutellaria galericulata	0.798	
	Thelypteris palustris	0.859	
Alnion incanae	*Circaea lutetiana*	0.735	0.735
	Festuca gigantea	0.729	
	Prunus padus	0.749	
	Stachys sylvatica	0.726	
Alnion viridis	*Alnus alnobetula*	0.957	0.934
	Ribes petraeum	0.884	
	Salix waldsteiniana	0.961	
Alysso alyssoidis-Sedion albi	*Alyssum alyssoides*	0.824	0.887
	Bombycilaena erecta	0.914	
	Bromus hordeaceus	0.777	
	Cerastium glutinosum	0.971	
	Cerastium pumilum	0.827	
	Cerastium tenoreanum	0.939	
	Hornungia petraea	0.951	
	Minuartia fastigiata	0.902	
	Minuartia mutabilis	0.928	
	Reseda phyteuma	0.941	
	Saxifraga tridactylites	0.818	
	Sedum sexangulare	0.748	
	Sideritis montana	0.963	
	Thlaspi perfoliatum	0.84	
	Trifolium scabrum	0.935	
	Veronica praecox	0.915	
Alysso saxatilis-Festucion pallentis	Allium senescens ssp. montanum	0.794	0.876
	Aurinia saxatilis ssp. saxatilis	0.952	
	Festuca pallens	0.829	
	Helianthemum nummularium	NA	

	Hieracium schmidtii	0.91	
	Sedum rupestre	0.79	
	Seseli osseum	0.978	
Arabidopsidion thalianae	Arabidopsis thaliana	0.789	0.881
	Valerianella carinata	0.928	
	Veronica dillenii	0.923	
	Veronica triphyllos	0.908	
	Veronica verna	0.858	
Arrhenatherion	Arrhenatherum elatius	NA	0.741
	Campanula patula	0.722	
	Crepis biennis	0.738	
	Galium album	NA	
	Pastinaca sativa	0.763	
	Pimpinella major	NA	
Betulion pubescentis	Betula pubescens	0.731	0.731
Bromion erecti	Aceras anthropophorum	0.955	0.87
	Colchicum autumnale	0.733	
	Euphrasia rostkoviana	0.749	
	Laserpitium siler	0.874	
	Linum viscosum	0.912	
	Listera ovata	NA	
	Melampyrum arvense	0.861	
	Onobrychis montana	0.947	
	Onobrychis viciifolia	0.788	
	Ophrys apifera	0.879	
	Ophrys holoserica	0.884	
	Ophrys insectifera	0.876	
	Ophrys sphegodes	0.871	
	Pedicularis comosa	0.958	
	Thesium humifusum	0.907	
	Tragopogon orientalis	0.855	
Bromo pannonici-Festucion pallentis	Aethionema saxatile	0.912	0.893
	Campanula sibirica	0.903	
	Echinops ritro ssp. ruthenicus	0.987	
	Fumana procumbens	0.787	
	Helianthemum canum	0.834	
	Helianthemum nummularium	NA	
	Lotus borbasii	0.986	
	Medicago orbicularis	0.975	
	Ononis pusilla	0.859	
	Poa badensis	NA	
	Rhamnus saxatilis	0.812	
	Scabiosa canescens	0.922	
	Scorzonera austriaca	0.882	
	Seseli hippomarathrum	0.937	
	Stipa pulcherrima	0.9	
	Viola rupestris	0.806	
Calamagrostion variae	Calamagrostis varia	0.878	0.862
	Gymnadenia odoratissima	0.863	

	Laserpitium siler	0.874	
	Molinia caerulea	0.747	
	Peucedanum verticillare	0.949	
Calthion	Bromus racemosus	0.881	0.805
	Caltha palustris	NA	
	Cirsium oleraceum	0.725	
	Crepis paludosa	0.798	
	Lotus pedunculatus	0.825	
	Myosotis palustris agg.	0.836	
	Scirpus sylvaticus	0.763	
Caricion atrofusco-saxatilis	Carex parallela	0.87	0.956
	Juncus triglumis	0.974	
	Kobresia simpliciuscula	0.991	
	Tofieldia pusilla	0.99	
Caricion austroalpinae	Allium ochroleucum	0.859	0.948
	Carex austroalpina	0.955	
	Festuca calva	0.978	
	Horminum pyrenaicum	0.962	
	Koeleria eriostachya	0.982	
	Laserpitium peucedanoides	0.971	
	Pedicularis gyroflexa	0.926	
Caricion curvulae	Carex brunnescens	0.985	0.98
	Carex curvula	0.985	
	Festuca halleri	0.981	
	Festuca pseudodura	0.992	
	Festuca supina	0.972	
	Hieracium glanduliferum	0.991	
	Minuartia recurva	0.943	
	Oreochloa disticha	0.987	
	Pedicularis kerneri	0.982	
	Senecio incanus ssp. carniolicus	0.988	
	Veronica bellidioides	0.977	
Caricion davallianae	Blysmus compressus	0.805	0.829
	Carex davalliana	0.765	
	Carex hostiana	0.843	
	Carex lepidocarpa	0.769	
	Carex pulicaris	0.796	
	Dactylorhiza incarnata	0.824	
	Dactylorhiza majalis	0.774	
	Epipactis palustris	0.78	
	Eriophorum latifolium	0.74	
	Liparis loeselii	0.951	
	Schoenus ferrugineus	0.926	
	Trichophorum alpinum	0.887	
	Triglochin palustre	0.911	
Caricion ferruginae	Alchemilla anisiaca	0.986	0.955
	Allium victorialis	0.956	
	Anemone baldensis	0.981	
	Anemone narcissiflora	0.975	

	Astragalus frigidus	0.988	
	Astrantia bavarica	0.977	
	Campanula thyrsoides	0.978	
	Carex ferruginea	0.945	
	Crepis mollis	0.851	
	Crepis pontana	0.975	
	Festuca norica	0.983	
	Festuca pulchella	0.969	
	Lathyrus laevigatus	0.916	
	Luzula glabrata	0.97	
	Pedicularis foliosa	0.965	
	Phleum hirsutum	0.926	
	Plantago atrata	0.946	
	Senecio doronicum	0.931	
	Traunsteinera globosa	0.896	
	Trifolium badium	0.963	
	Trifolium pratense ssp. nivale	0.974	
	Trifolium thalii	0.953	
Caricion firmae	Androsace chamaejasme	0.974	0.975
	Carex firma	0.96	
	Chamorchis alpina	0.982	
	Crepis jacquinii	0.943	
	Crepis kerneri	0.981	
	Festuca pumila	0.977	
	Helianthemum alpestre	0.979	
	Minuartia gerardii	0.979	
	Pedicularis portenschlagii	0.996	
	Pedicularis rosea	0.984	
	Saussurea pygmaea	0.98	
	Saxifraga caesia	0.962	
Caricion fuscae	Agrostis canina	0.75	0.8
	Carex canescens	0.843	
	Carex echinata	0.794	
	Carex hartmanii	0.889	
	Carex nigra	0.771	
	Epilobium palustre	0.746	
	Juncus filiformis	0.811	
	Viola palustris	0.797	
Caricion lasiocarpae	Carex lasiocarpa	0.831	0.807
	Carex rostrata	0.782	
	Menyanthes trifoliata	0.767	
	Pedicularis palustris	0.831	
	Potentilla palustris	0.826	
Carpinion betuli	Carex pilosa	0.761	0.795
	Carpinus betulus	0.739	
	Festuca heterophylla	0.981	
	Fragaria moschata	0.769	
	Galium sylvaticum	0.766	
	Lathyrus niger	0.776	

	Prunus avium	0.73	
	Rosa arvensis	0.792	
	Stellaria holostea	0.761	
	Viola alba	0.877	
	Viola riviniana	NA	
Caricion firmae	Androsace chamaejasme	0.974	0.975
	Carex firma	0.96	
	Chamorchis alpina	0.982	
	Crepis jacquinii	0.943	
	Crepis kerneri	0.981	
	Festuca pumila	0.977	
	Helianthemum alpestre	0.979	
	Minuartia gerardii	0.979	
	Pedicularis portenschlagii	0.996	
	Pedicularis rosea	0.984	
	Saussurea pygmaea	0.98	
	Saxifraga caesia	0.962	
Caricion fuscae	Agrostis canina	0.75	0.8
	Carex canescens	0.843	
	Carex echinata	0.794	
	Carex hartmanii	0.889	
	Carex nigra	0.771	
	Epilobium palustre	0.746	
	Juncus filiformis	0.811	
	Viola palustris	0.797	
Caricion lasiocarpae	Carex lasiocarpa	0.831	0.807
	Carex rostrata	0.782	
	Menyanthes trifoliata	0.767	
	Pedicularis palustris	0.831	
	Potentilla palustris	0.826	
Carpinion betuli	Carex pilosa	0.761	0.795
	Carpinus betulus	0.739	
	Festuca heterophylla	0.981	
	Fragaria moschata	0.769	
	Galium sylvaticum	0.766	
	Lathyrus niger	0.776	
	Prunus avium	0.73	
	Rosa arvensis	0.792	
	Stellaria holostea	0.761	
	Viola alba	0.877	
	Viola riviniana	NA	
Diantho lumnitzeri-Seslerion	Acinos alpinus	0.829	0.891
	Anthyllis montana ssp. jacquinii	0.983	
	Betonica alopecuros	0.941	
	Buphthalmum salicifolium	0.854	
	Carduus crassifolius	NA	
	Erysimum sylvestre	0.914	
	Euphrasia salisburgensis	0.927	
	Galium lucidum	0.781	

	Globularia cordifolia	0.842	
	Hippocrepis comosa	0.742	
	Leontodon incanus	0.794	
	Micromeria thymifolia	0.987	
	Minuartia setacea	0.952	
	Phyteuma orbiculare	0.866	
	Pleurospermum austriacum	0.893	
	Saxifraga paniculata	0.925	
	Seseli austriacum	0.958	
	Sesleria albicans	0.84	
	Sesleria heuflerana	0.986	
	Thalictrum foetidum	NA	
	Thlaspi montanum	0.911	
Ericion carneae	Daphne striata	0.966	0.967
	Genista radiata	0.968	
Erico-Pinion sylvestris	Aquilegia atrata	0.926	0.884
	Coronilla vaginalis	0.836	
	Daphne cneorum	0.839	
	Festuca amethystina	0.912	
	Leontodon incanus	0.794	
	Thesium rostratum	0.995	
Euphorbio-Callunion	Agrostis vinealis	0.918	0.862
	Avenula pratensis	0.835	
	Dactylorhiza sambucina	0.88	
	Festuca heteropachys	0.745	
	Genista sagittalis	0.955	
	Hieracium peletierianum	0.915	
	Saxifraga granulata	0.784	
Fagion sylvaticae	Euphorbia amygdaloides	NA	0.788
	Fagus sylvatica	0.725	
	Festuca altissima	0.814	
	Neottia nidus-avis	NA	
	Prenanthes purpurea	0.824	
Festucion pseudovinae	Achillea aspleniifolia	0.999	0.979
	Artemisia santonicum	0.996	
	Bupleurum tenuissimum	0.984	
	Eryngium planum	0.98	
	Gypsophila muralis	0.934	
Festucion vaginatae	Dianthus diutinus	0.974	0.96
	Festuca vaginata	0.961	
	Gypsophila fastigiata	0.944	
	Gypsophila paniculata	0.996	
	Helichrysum arenarium	0.936	
	Koeleria glauca	0.949	
Festucion valesiacae	Achillea pannonica	0.919	0.938
	Adonis vernalis	0.933	
	Astragalus vesicarius	0.949	
	Carduus collinus	0.927	
	Carex supina	0.961	

	Centaurea biebersteinii	0.981	
	Chamaecytisus austriacus	0.941	
	Chondrilla juncea	0.858	
	Crepis nicaeensis	0.991	
	Erysimum andrzejowskianum	0.967	
	Euphorbia glareosa	0.998	
	Euphrasia pectinata	0.948	
	Euphrasia stricta	NA	
	Festuca duvalii	0.988	
	Festuca pseudodalmatica	0.894	
	Inula oculus-christi	0.96	
	Iris aphylla	0.976	
	Iris pumila	0.95	
	Isatis tinctoria	0.871	
	Lactuca viminea	0.872	
	Linum austriacum	0.951	
	Medicago prostrata	0.955	
	Minuartia glaucina	0.835	
	Muscari comosum	0.868	
	Muscari neglectum	0.814	
	Muscari tenuiflorum	0.947	
	Nonea pulla	0.952	
	Ornithogalum kochii	0.982	
	Ornithogalum pannonicum	0.967	
	Pseudolysimachion orchideum	0.92	
	Ranunculus illyricus	0.881	
	Rapistrum perenne	0.975	
	Salvia nemorosa	0.951	
	Thymus kosteletzkyanus	0.925	
	Thymus odoratissimus	0.97	
	Vinca herbacea	0.992	
	Viola ambigua	0.964	
	Xeranthemum cylindraceum	0.978	
Festucion variae	Festuca varia	0.987	0.94
	Hieracium hoppeanum	0.832	
	Pedicularis tuberosa	0.986	
	Potentilla grandiflora	0.957	
Fraxino orni-Ostryion	Acer obtusatum	0.961	0.913
	Asparagus tenuifolius	0.95	
	Carpinus orientalis	0.972	
	Dianthus monspessulanus	0.928	
	Fraxinus ornus	0.872	
	Laburnum anagyroides	0.868	
	Lilium bulbiferum	0.854	
	Ostrya carpinifolia	0.901	
Genistion pilosae	Calluna vulgaris	NA	0.852
	Genista anglica	0.856	
	Genista germanica	0.804	
	Genista pilosa	NA	

	Genista sagittalis	0.955	
	Lycopodium clavatum	0.793	
Hyperico perforati-Scleranthion perennis	Aira caryophyllea	0.858	0.855
	Festuca ovina	NA	
	Scleranthus perennis	0.852	
Juncion trifidi	Juncus trifidus	0.979	0.987
	Senecio carpaticus	0.995	
Koelerion arenariae	Cerastium semidecandrum	0.788	0.91
	Equisetum ramosissimum	0.957	
	Phleum arenarium	0.945	
	Silene conica	0.949	
Loiseleurio-Vaccinion	Empetrum hermaphroditum	0.985	0.984
	Loiseleuria procumbens	0.982	
Molinion	Achillea aspleniifolia	0.999	0.841
	Carex tomentosa	0.783	
	Dianthus superbus	0.89	
	Euphrasia kerneri	0.994	
	Galium boreale	0.782	
	Gentiana pneumonanthe	0.806	
	Gentianella austriaca	0.931	
	Gladiolus palustris	0.965	
	Inula salicina	0.77	
	Iris sibirica	0.829	
	Laserpitium prutenicum	0.883	
	Molinia caerulea	0.747	
	Ophioglossum vulgatum	0.833	
	Scorzonera humilis	0.76	
	Selinum carvifolia	0.772	
	Serratula tinctoria	0.773	
	Silaum silaus	0.868	
	Succisa pratensis	0.745	
Nardion strictae	Ajuga pyramidalis	0.942	0.966
	Campanula barbata	0.95	
	Geum montanum	0.975	
	Pseudorchis albida	0.964	
	Ranunculus villarsii	0.996	
	Viola lutea ssp. sudetica	0.969	
Nardo-Agrostion tenuis	Avenula planiculmis	0.987	0.912
	Campanula serrata	0.959	
	Carex leporina	0.791	
	Gentiana pannonica	0.967	
	Gnaphalium sylvaticum	0.821	
	Hieracium aurantiacum	0.947	
Nardo-Juncion squarrosi	Juncus squarrosus	0.827	0.844
	Pedicularis sylvatica	0.862	
Ononido rotundfolii-Pinion sylvestris	Astragalus monspessulanus	0.925	0.943
	Ononis rotundifolia	0.961	
Oxyococco-Empetrion hermaphroditi	Betula nana	0.921	0.929
	Vaccinium microcarpum	0.937	

Oxytropido-Elynion	Antennaria carpatica	0.976	0.978
	Astragalus alpinus	0.981	
	Astragalus australis	0.965	
	Carex capillaris	0.965	
	Carex rupestris	0.975	
	Comastoma tenellum	0.983	
	Dryas octopetala	0.957	
	Erigeron uniflorus	0.989	
	Kobresia myosuroides	0.99	
	Lloydia serotina	0.986	
	Oxytropis triflora	0.999	
	Pedicularis oederi	0.99	
	Potentilla crantzii	0.95	
	Salix serpillifolia	0.982	
Phyteumo-Trisetion	Cardaminopsis halleri	0.873	0.866
	Chaerophyllum aureum	0.824	
	Poa chaixii	0.9	
Pinion mugi	Larix decidua	0.867	0.933
	Pinus cembra	0.966	
	Pinus mugo	0.943	
	Pinus uncinata	0.934	
	Sorbus chamaemespilus	0.957	
Poion alpinae	Crepis aurea	0.969	0.962
	Phleum rhaeticum	0.968	
	Plantago alpina	0.949	
	Poa alpina	0.962	
	Trifolium badium	0.963	
Alliance	**Species**	**EM_ROC**	**meanROC**
Polygono-Trisetion	Centaurea pseudophrygia	0.931	0.893
	Crocus albiflorus	0.929	
	Persicaria bistorta	0.867	
	Trollius europaeus	0.845	
Quercion pubescenti-petrae	Betonica officinalis	0.862	0.863
	Bupleurum falcatum	0.766	
	Campanula bononiensis	0.852	
	Carex michelii	0.88	
	Clematis recta	0.859	
	Euphorbia polychroma	0.982	
	Fragaria viridis	0.822	
	Hierochloe australis	0.937	
	Inula hirta	0.848	
	Peucedanum alsaticum	0.921	
	Potentilla alba	0.843	
	Ranunculus polyanthemos	0.788	
	Serratula tinctoria	0.773	
	Vicia cassubica	0.865	
	Viola suavis	0.953	
Quercion roboris	Hieracium lachenalii	0.897	0.81
	Hieracium laevigatum	0.801	

	Hieracium racemosum	0.77	
	Lathyrus linifolius	0.762	
	Melampyrum pratense	NA	
	Teucrium scorodonia	0.818	
Rhododendro-Vaccinion	Rhododendron ferrugineum	0.975	0.975
Rhynchosporion albae	Carex limosa	0.84	0.876
	Drosera anglica	0.923	
	Drosera intermedia	0.913	
	Rhynchospora alba	0.828	
Salicion auritae	Salix aurita	0.775	0.88
	Salix repens	0.984	
Salicion cinerae	Salix cinerea	0.745	0.745
Salicion eleagno-daphnoidis	Salix daphnoides	0.958	0.928
	Salix eleagnos	0.913	
	Salix myrsinifolia	0.913	
Salicion purpureae	Salix purpurea	NA	NA
Scorzonero-Juncion gerardii	Carex distans	0.825	0.936
	Carex divisa	0.961	
	Carex otrubae	0.871	
	Cirsium brachycephalum	0.989	
	Glaux maritima	0.949	
	Juncus gerardii	0.952	
	Lotus maritimus	0.977	
	Samolus valerandi	0.965	
	Taraxacum bessarabicum	0.992	
	Trifolium fragiferum	0.85	
	Triglochin maritimum	0.965	
Sedo-Scleranthion biennis	Cerastium arvense ssp. strictum	0.967	0.915
	Dianthus sylvestris	0.859	
	Petrorhagia saxifraga	0.816	
	Sedum annuum	0.94	
	Sempervivum arachnoideum	0.927	
	Sempervivum montanum	0.963	
	Sempervivum tectorum	0.865	
	Silene rupestris	0.94	
	Veronica fruticans	0.957	
Seslerion coeruleae	Arabis ciliata	0.951	0.922
	Aster alpinus	0.894	
	Bupleurum ranunculoides	0.927	
	Carex ornithopoda	0.865	
	Dianthus alpinus	0.984	
	Gentiana utriculosa	0.91	
Sphagnion medii	Vaccinium oxycoccos	0.847	0.847
Stipo-Poion xerophilae	Centaurea maculosa	0.906	0.922
	Minuartia laricifolia	0.963	
	Poa molinerii	0.955	
	Thymus pulegioides ssp. carniolicus	0.863	
Thero-Airion	Aira caryophyllea	0.858	0.924
	Aira elegans	0.981	

	Aira praecox	0.976	
	Filago minima	0.848	
	Filago pyramidata	0.962	
	Filago vulgaris	0.938	
	Hypochoeris glabra	0.959	
	Moenchia mantica	0.925	
	Myosotis discolor	0.887	
	Ornithopus perpusillus	0.852	
	Trifolium striatum	0.83	
	Tuberaria guttata	0.996	
	Ventenata dubia	0.995	
Tilio-Acerion	Acer platanoides	0.73	0.793
	Acer pseudoplatanus	0.714	
	Aruncus dioicus	0.83	
	Asperula taurina	0.884	
	Campanula latifolia	0.85	
	Euonymus latifolia	0.848	
	Geranium robertianum	NA	
	Lunaria rediviva	0.82	
	Ribes uva-crispa	0.777	
	Staphylea pinnata	0.793	
	Tilia platyphyllos	0.74	
	Ulmus glabra	0.742	
Vaccinio uliginosi-Pinion sylvestris	Ledum palustre	0.92	0.893
	Vaccinium uliginosum	0.865	
Violion caninae	Centaurea nigra	0.832	0.826
	Dianthus armeria	0.84	
	Dianthus deltoides	0.79	
	Galium pumilum	0.726	
	Jasione laevis	0.941	
	Polygala vulgaris	NA	
	Viola canina	NA	

Tab.3 Projected alliances‘probability of occurrence upon the ecological space spanned by increasing temperature (= x) and decreasing precipitation (= y)

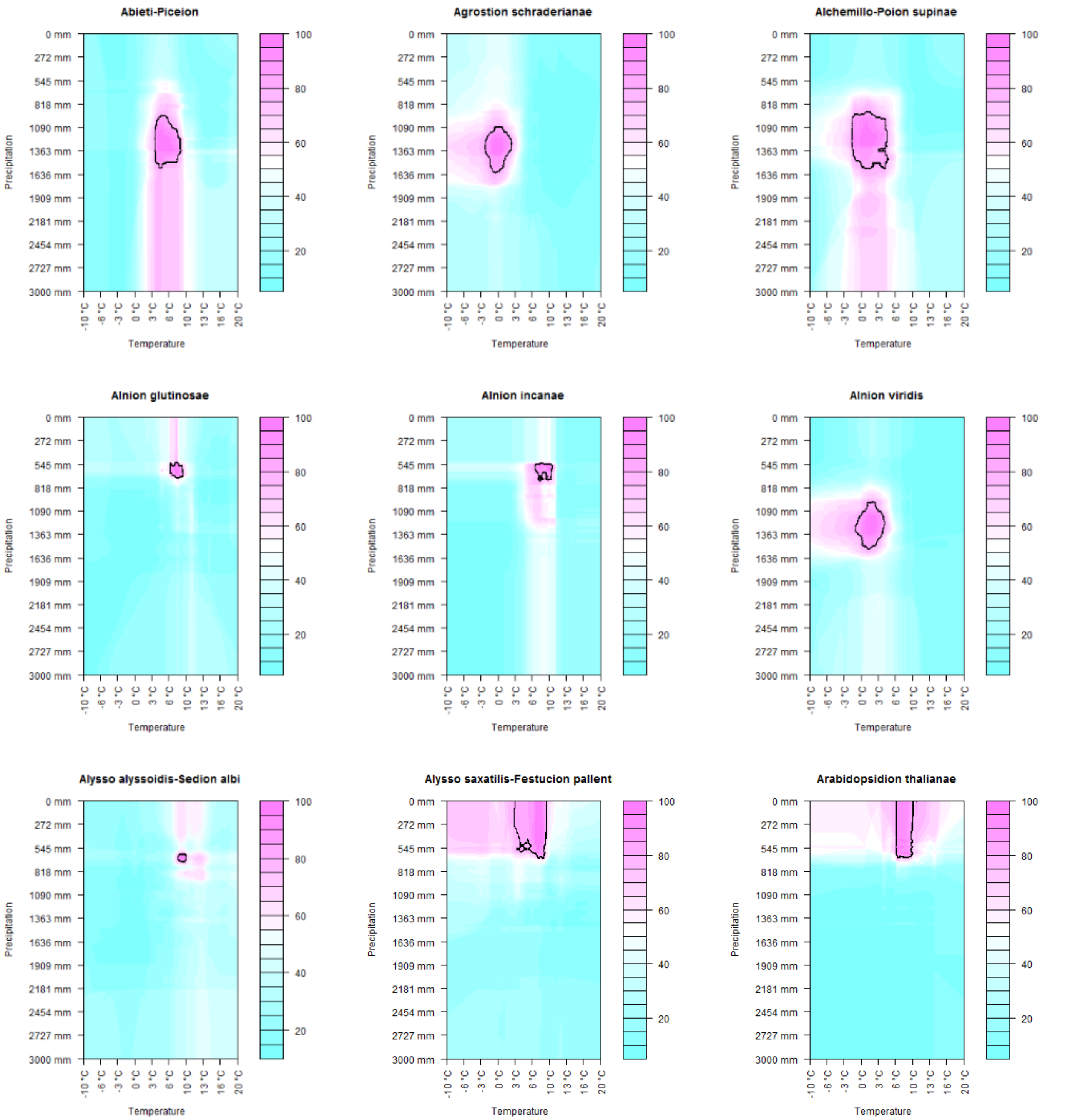

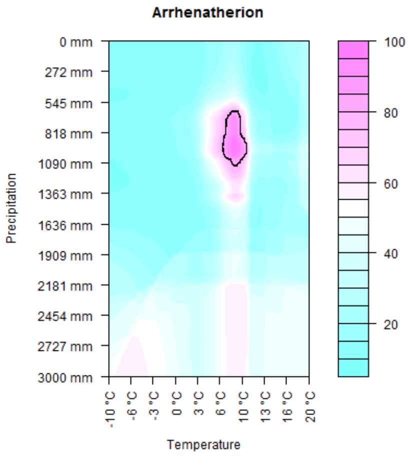
Arrhenatherion
0 mm 272 mm 545 mm 818 mm 1090 mm 1363 mm 1636 mm 1909 mm 2181 mm 2454 mm 2727 mm 3000 mm
Precipitation
-10 °C -6 °C -3 °C 0 °C 3 °C 6 °C 10 °C 13 °C 16 °C 20 °C
Temperature
100 80 60 40 20

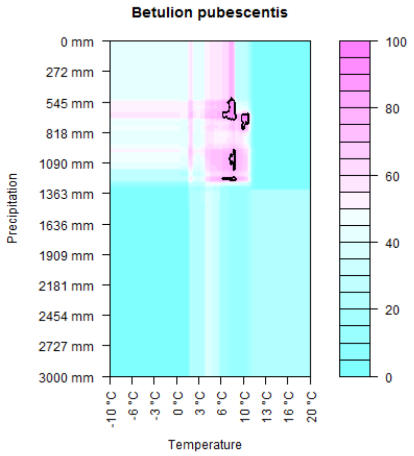
Betulion pubescentis
0 mm 272 mm 545 mm 818 mm 1090 mm 1363 mm 1636 mm 1909 mm 2181 mm 2454 mm 2727 mm 3000 mm
Precipitation
-10 °C -6 °C -3 °C 0 °C 3 °C 6 °C 10 °C 13 °C 16 °C 20 °C
Temperature
100 80 60 40 20 0

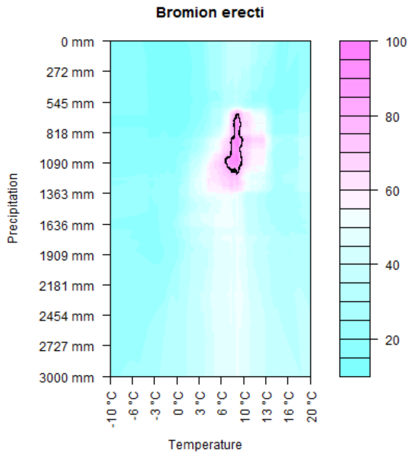
Bromion erecti
0 mm 272 mm 545 mm 818 mm 1090 mm 1363 mm 1636 mm 1909 mm 2181 mm 2454 mm 2727 mm 3000 mm
Precipitation
-10 °C -6 °C -3 °C 0 °C 3 °C 6 °C 10 °C 13 °C 16 °C 20 °C
Temperature
100 80 60 40 20

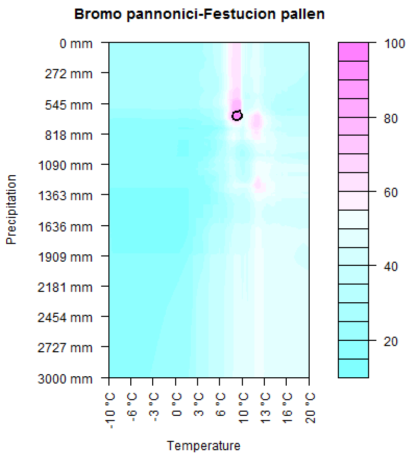
Bromo pannonici-Festucion pallen
0 mm 272 mm 545 mm 818 mm 1090 mm 1363 mm 1636 mm 1909 mm 2181 mm 2454 mm 2727 mm 3000 mm
Precipitation
-10 °C -6 °C -3 °C 0 °C 3 °C 6 °C 10 °C 13 °C 16 °C 20 °C
Temperature
100 80 60 40 20

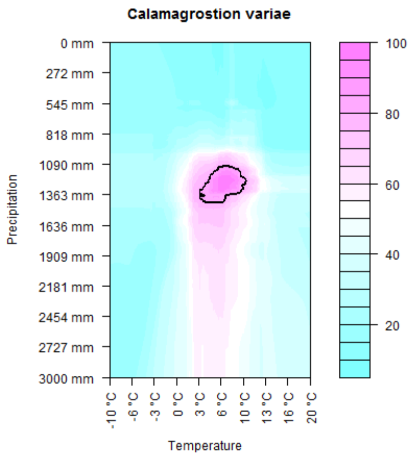
Calamagrostion variae
0 mm 272 mm 545 mm 818 mm 1090 mm 1363 mm 1636 mm 1909 mm 2181 mm 2454 mm 2727 mm 3000 mm
Precipitation
-10 °C -6 °C -3 °C 0 °C 3 °C 6 °C 10 °C 13 °C 16 °C 20 °C
Temperature
100 80 60 40 20

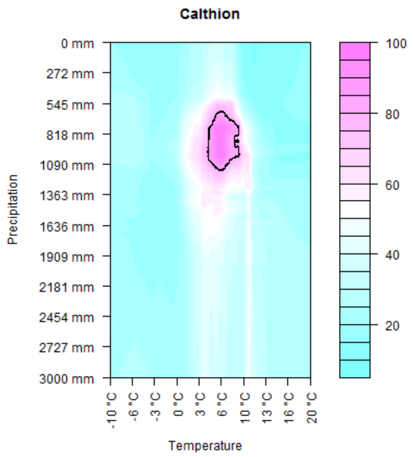
Calthion
0 mm 272 mm 545 mm 818 mm 1090 mm 1363 mm 1636 mm 1909 mm 2181 mm 2454 mm 2727 mm 3000 mm
Precipitation
-10 °C -6 °C -3 °C 0 °C 3 °C 6 °C 10 °C 13 °C 16 °C 20 °C
Temperature
100 80 60 40 20

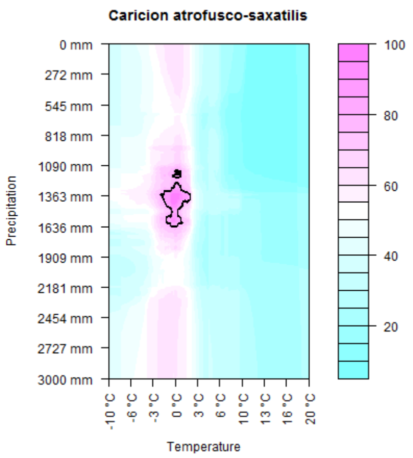
Caricion atrofusco-saxatilis
0 mm 272 mm 545 mm 818 mm 1090 mm 1363 mm 1636 mm 1909 mm 2181 mm 2454 mm 2727 mm 3000 mm
Precipitation
-10 °C -6 °C -3 °C 0 °C 3 °C 6 °C 10 °C 13 °C 16 °C 20 °C
Temperature
100 80 60 40 20

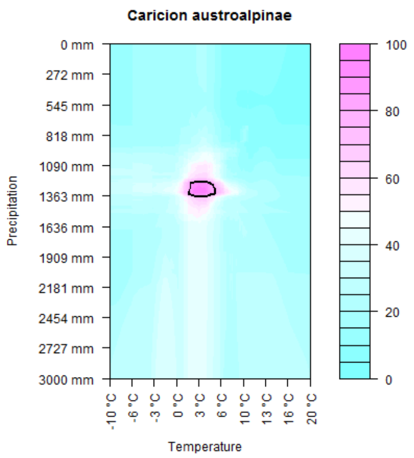
Caricion austroalpinae
0 mm 272 mm 545 mm 818 mm 1090 mm 1363 mm 1636 mm 1909 mm 2181 mm 2454 mm 2727 mm 3000 mm
Precipitation
-10 °C -6 °C -3 °C 0 °C 3 °C 6 °C 10 °C 13 °C 16 °C 20 °C
Temperature
100 80 60 40 20 0

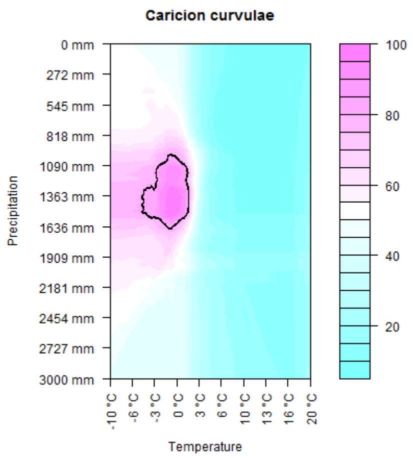
Caricion curvulae
0 mm 272 mm 545 mm 818 mm 1090 mm 1363 mm 1636 mm 1909 mm 2181 mm 2454 mm 2727 mm 3000 mm
Precipitation
-10 °C -6 °C -3 °C 0 °C 3 °C 6 °C 10 °C 13 °C 16 °C 20 °C
Temperature
100 80 60 40 20

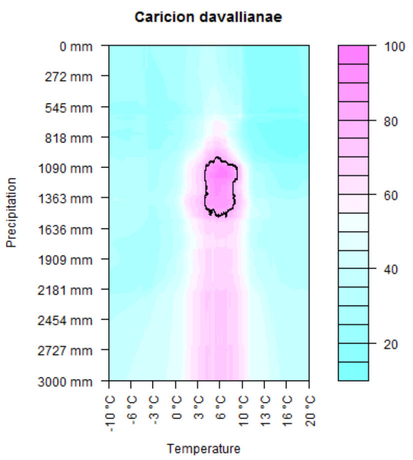
Caricion davallianae
0 mm 272 mm 545 mm 818 mm 1090 mm 1363 mm 1636 mm 1909 mm 2181 mm 2454 mm 2727 mm 3000 mm
Precipitation
-10 °C -6 °C -3 °C 0 °C 3 °C 6 °C 10 °C 13 °C 16 °C 20 °C
Temperature
100 80 60 40 20

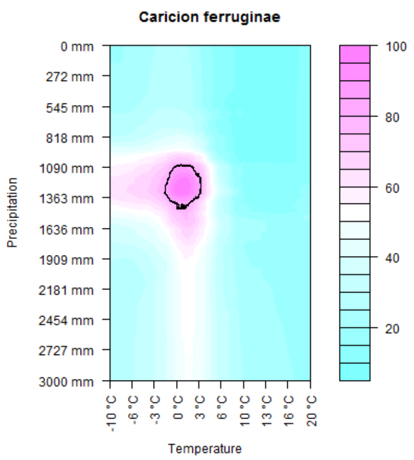
Caricion ferruginae
0 mm 272 mm 545 mm 818 mm 1090 mm 1363 mm 1636 mm 1909 mm 2181 mm 2454 mm 2727 mm 3000 mm
Precipitation
-10 °C -6 °C -3 °C 0 °C 3 °C 6 °C 10 °C 13 °C 16 °C 20 °C
Temperature
100 80 60 40 20

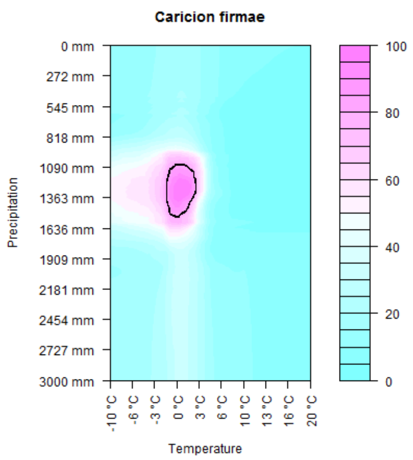
Caricion firmae
0 mm 272 mm 545 mm 818 mm 1090 mm 1363 mm 1636 mm 1909 mm 2181 mm 2454 mm 2727 mm 3000 mm
Precipitation
-10 °C -6 °C -3 °C 0 °C 3 °C 6 °C 10 °C 13 °C 16 °C 20 °C
Temperature
100 80 60 40 20 0

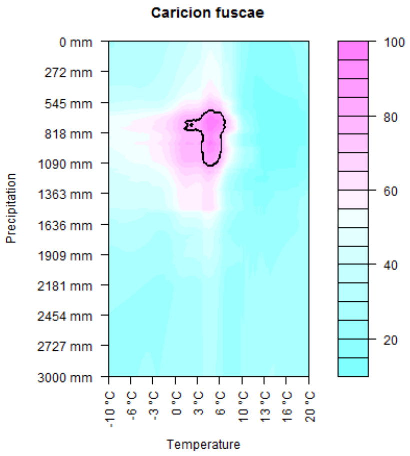
Caricion fuscae
Precipitation
Temperature

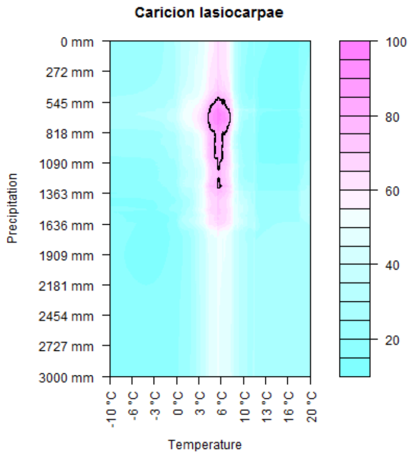
Caricion lasiocarpae
Precipitation
Temperature

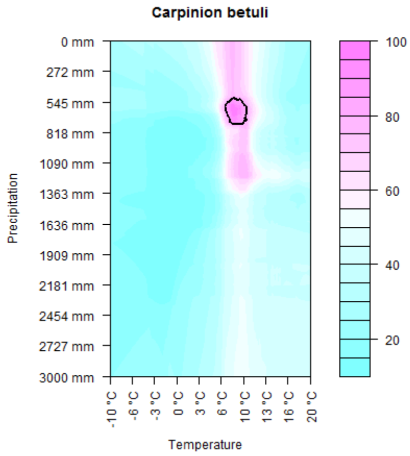
Carpinion betuli
Precipitation
Temperature

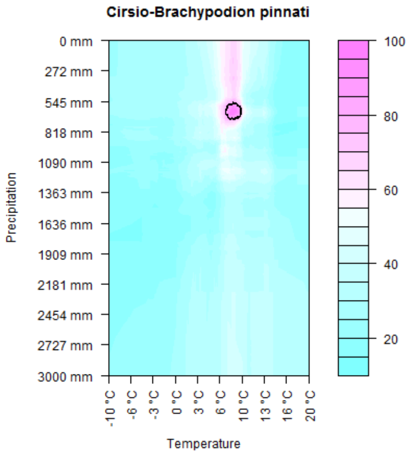
Cirsio-Brachypodion pinnati
Precipitation
Temperature

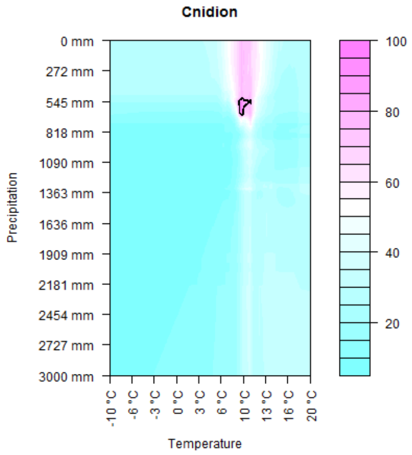
Cnidion
Precipitation
Temperature

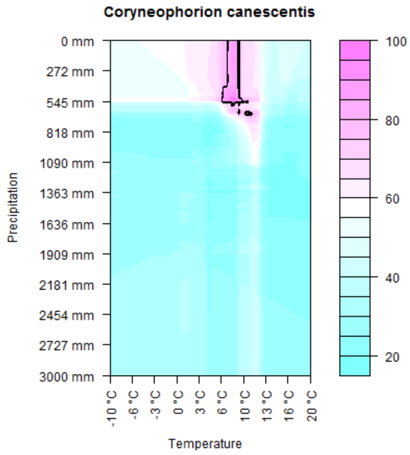
Coryneophorion canescentis
Precipitation
Temperature

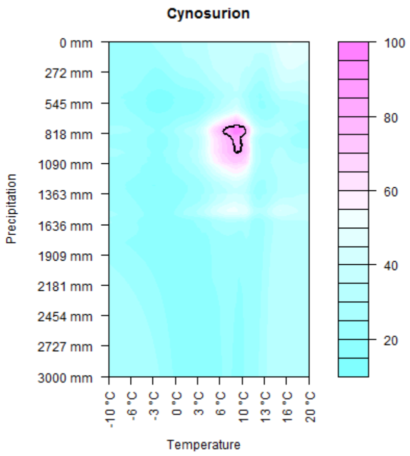
Cynosurion
Precipitation
Temperature

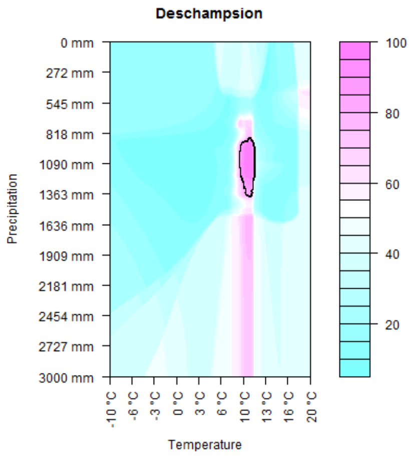
Deschampsion
Precipitation
Temperature

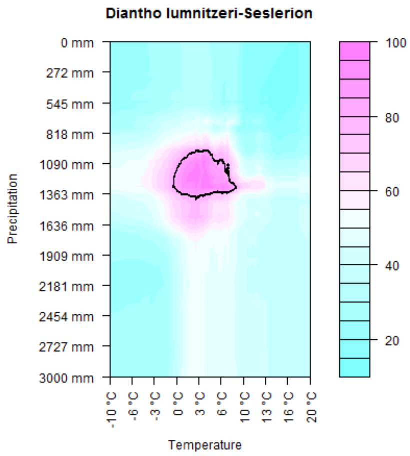
Diantho lumnitzeri-Seslerion
Precipitation
Temperature

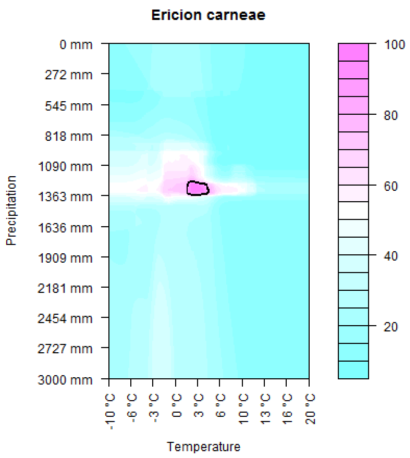
Ericion carneae
Precipitation
Temperature

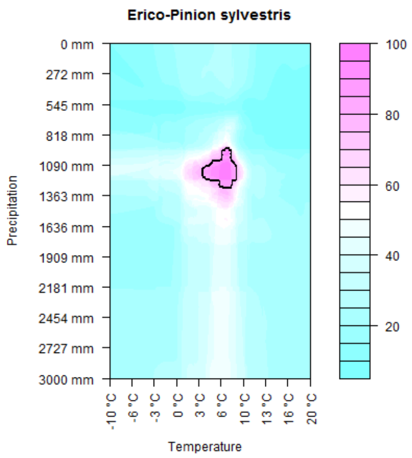
Erico-Pinion sylvestris
Precipitation
Temperature

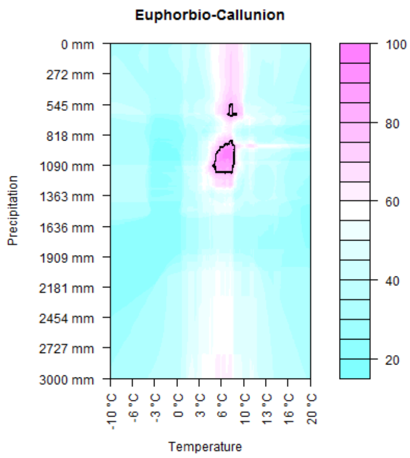
Euphorbio-Callunion
Precipitation
Temperature

Fagion sylvaticae

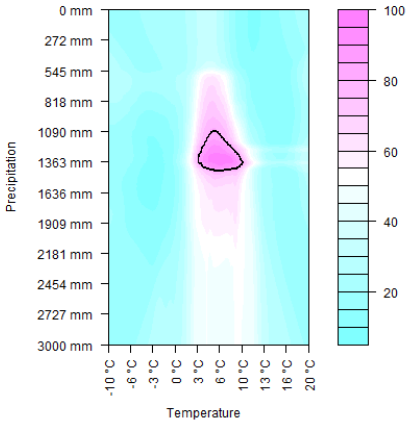

Festucion pseudovinae

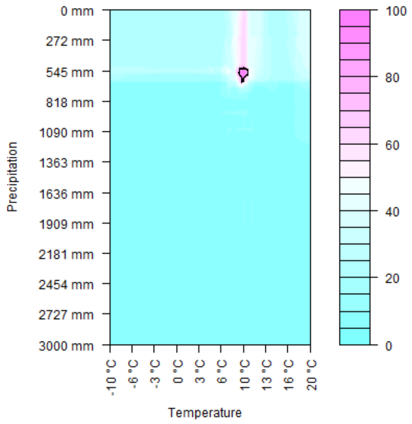

Festucion vaginatae

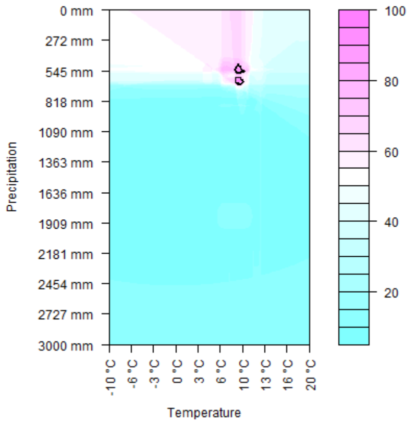

Festucion valesiacae

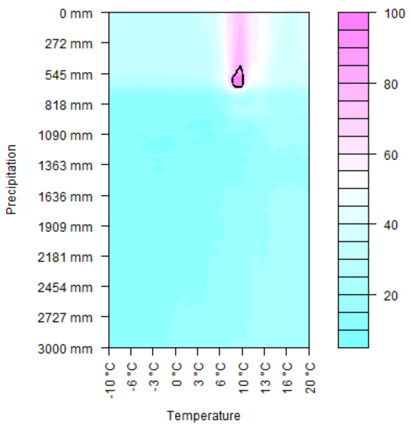

Festucion variae

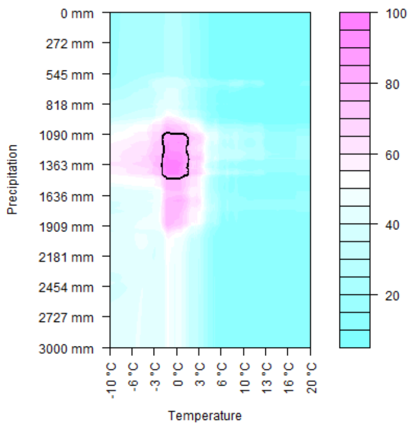

Fraxino orni-Ostryion

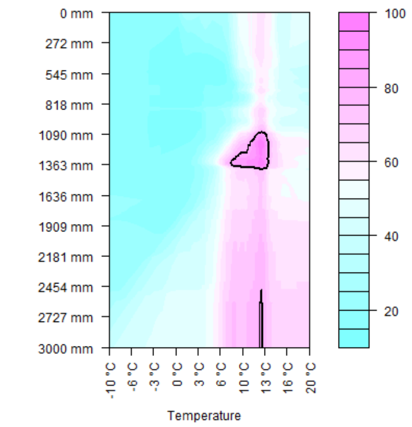

Genistion pilosae

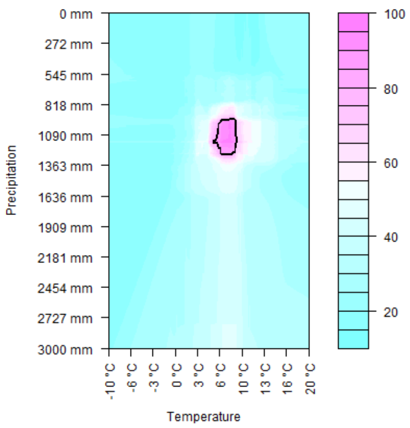

Hyperico perforati-Scleranthion pere

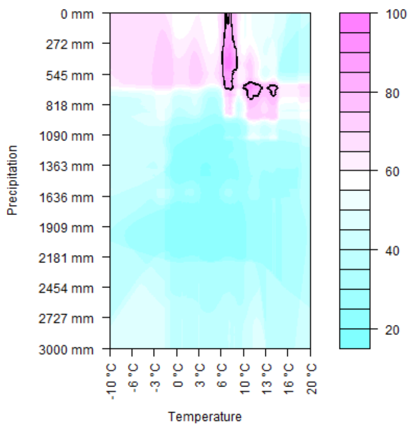

Juncion trifidi

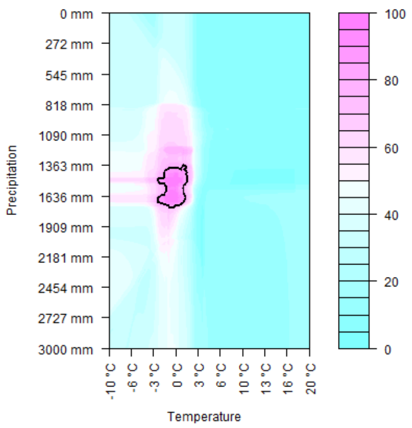

Koelerion arenariae

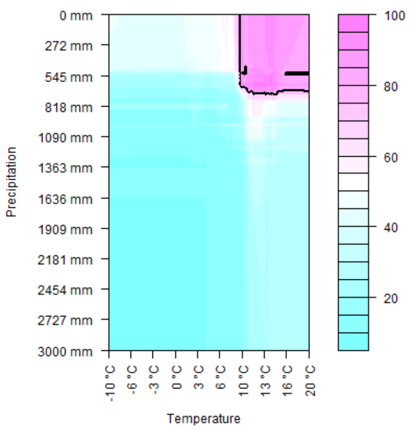

Loiseleurio-Vaccinion

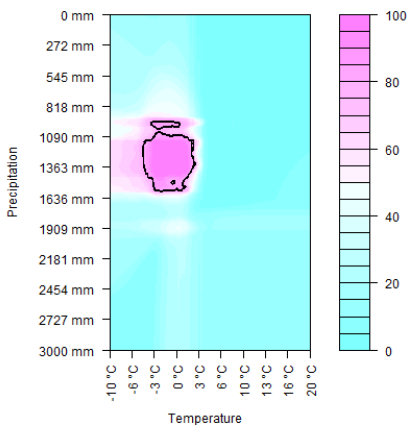

Molinion

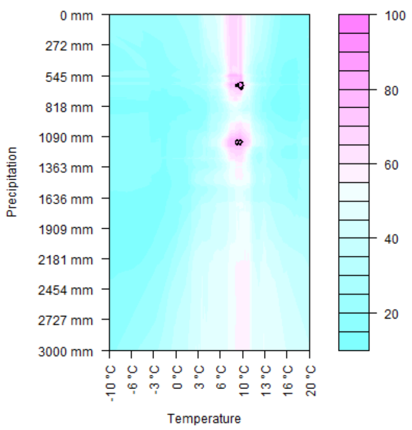


Nardion strictae
Nardo-Agrostion tenuis
Nardo-Juncion squarrosi
Ononido rotundfolii-Pinion sylvest
Oxyococco-Empetrion hermaphroc
Oxytropido-Elynion
Phyteumo-Trisetion
Pinion mugi
Poion alpinae
Polygono-Trisetion
Quercion pubescenti-petrae
Quercion roboris
Precipitation
0 mm
272 mm
545 mm
818 mm
1090 mm
1363 mm
1636 mm
1909 mm
2181 mm
2454 mm
2727 mm
3000 mm
Temperature
-10 °C
-6 °C
-3 °C
0 °C
3 °C
6 °C
10 °C
13 °C
16 °C
20 °C
0
20
40
60
80
100


Rhododendro-Vaccinion
Rhynchosporion albae
Salicion auritae
Salicion cinerae
Salicion eleagno-daphnoidis
Salicion purpureae
Scorzonero-Juncion gerardii
Sedo-Scleranthion biennis
Seslerion coeruleae
Sphagnion medii
Stipo-Poion xerophilae
Thero-Airion
Precipitation
0 mm
272 mm
545 mm
818 mm
1090 mm
1363 mm
1636 mm
1909 mm
2181 mm
2454 mm
2727 mm
3000 mm
Temperature
-10 °C
-6 °C
-3 °C
0 °C
3 °C
6 °C
10 °C
13 °C
16 °C
20 °C
0
20
40
60
80
100

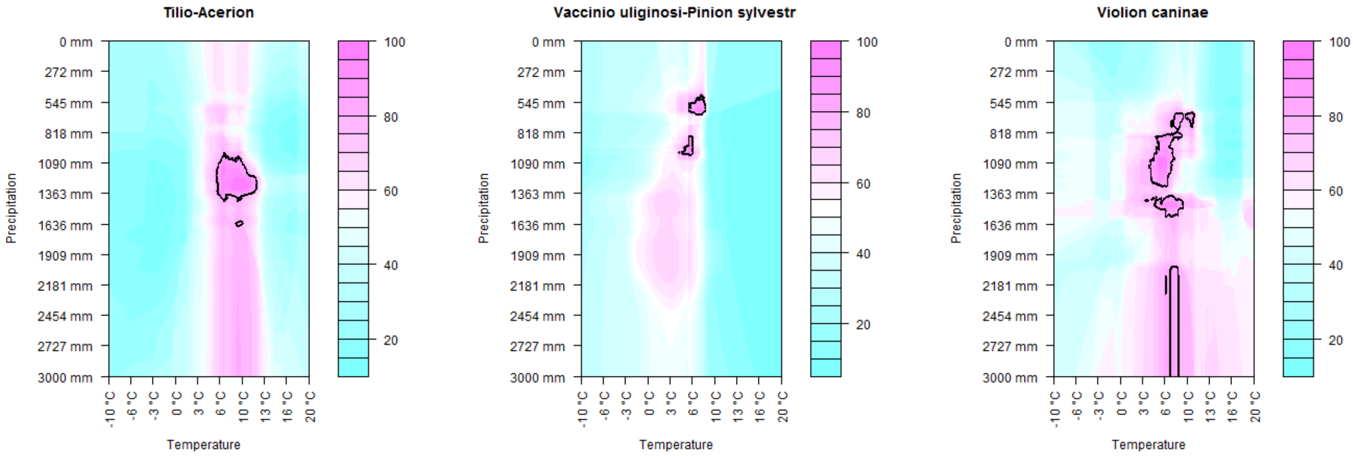

Tilio-Acerion
Vaccinio uliginosi-Pinion sylvestr
Violion caninae
Precipitation
0 mm
272 mm
545 mm
818 mm
1090 mm
1363 mm
1636 mm
1909 mm
2181 mm
2454 mm
2727 mm
3000 mm
Temperature
-10 °C
-6 °C
-3 °C
0 °C
3 °C
6 °C
10 °C
13 °C
16 °C
20 °C
100
80
60
40
20

Tab.4. Kruskal Wallis tests with single factor and combined risk as response and time, climate scenarios and N deposition scenarios as grouping factors.

RESPONSE	GROUPING FACTOR	CHI SQUARED	DF	P	
COMBINED RISK	**TIME**	32561	2	<0.0001	***
COMBINED RISK	**CLIMATE SCENARIOS**	40095	2	<0.0001	***
COMBINED RISK	**N DEPOSITION SCENARIOS**	526590	2	<0.0001	***
COMBINED RISK	**EUNIS CATEGORIES**	3091800	10	<0.0001	***
RISK OF WARMING	**TIME**	62091	2	<0.0001	***
RISK OF WARMING	**CLIMATE SCENARIOS**	100290	2	<0.0001	***
RISK OF WARMING	**EUNIS CATEGORIES**	796250	10	<0.0001	***
RISK OF DROUGHT	**TIME**	24289	2	<0.0001	***
RISK OF DROUGHT	**CLIMATE SCENARIOS**	29800	2	<0.0001	***
RISK OF DROUGHT	**EUNIS CATEGORIES**	920270	10	<0.0001	***
RISK OF N EXCEEDANCE	**TIME**	59853	2	<0.0001	***
RISK OF N EXCEEDANCE	**N DEPOSITION SCENARIOS**	655780	2	<0.0001	***
RISK OF N EXCEEDANCE	**EUNIS CATEGORIES**	2407900	10	<0.0001	***

Tab.5. Dunn's Test pairwise comparison of combined risk levels by time, climate scenarios and N deposition scenarios

PAIRWISE COMPARISON	Z- STATISTIC	P.ADJUSTED	P	
2010 - 2030	173.87500	< 0.001	< 0.001	***
2010 - 2050	169.84732	< 0.001	< 0.001	***
2030 - 2050	-7.53509	< 0.001	< 0.001	***
RCP26 - RCP85	195.63299	< 0.001	< 0.001	***
RCP26 - CURRENT	148.76316	< 0.001	< 0.001	***
RCP85 - CURRENT	-87.68542	< 0.001	< 0.001	***
N2010 - CLE2030	430.5210	< 0.001	< 0.001	***
N2010 - MFR2030	-269.5153	< 0.001	< 0.001	***
CLE2030 - MFR2030	-723.3242	< 0.001	< 0.001	***

Tab.6 Dunn's Test pairwise comparison of **combined risk** levels by EUNIS level 2 habitat categories.

PAIRWISE COMPARISON	Z- STATISTIC	P.ADJUSTED	P	
G3 - E2	-7.5701832	< 0.001	< 0.001	***
G3 - G1	48.3040381	< 0.001	< 0.001	***
E2 - G1	52.4146509	< 0.001	< 0.001	***
G3 - E4	21.9178592	< 0.001	< 0.001	***
E2 - E4	28.7005723	< 0.001	< 0.001	***
G1 - E4	-38.2228535	< 0.001	< 0.001	***
G3 - F2	101.9246394	< 0.001	< 0.001	***
E2 - F2	98.7954587	< 0.001	< 0.001	***
G1 - F2	56.7175151	< 0.001	< 0.001	***
E4 - F2	140.6096611	< 0.001	< 0.001	***
G3 - D2	76.2872236	< 0.001	< 0.001	***
E2 - D2	77.8301689	< 0.001	< 0.001	***
G1 - D2	32.7730564	< 0.001	< 0.001	***
E4 - D2	76.5586914	< 0.001	< 0.001	***
F2 - D2	-11.7025383	< 0.001	< 0.001	***
G3 - E3	-35.2670262	< 0.001	< 0.001	***
E2 - E3	-20.7114881	< 0.001	< 0.001	***
G1 - E3	-128.4193711	< 0.001	< 0.001	***
E4 - E3	-109.5500348	< 0.001	< 0.001	***
F2 - E3	-1357.5946055	< 0.001	< 0.001	***
D2 - E3	-179.7225529	< 0.001	< 0.001	***
G3 - D1	11.9141469	< 0.001	< 0.001	***
E2 - D1	20.3832898	< 0.001	< 0.001	***
G1 - D1	-64.4836327	< 0.001	< 0.001	***
E4 - D1	-23.4352639	< 0.001	< 0.001	***
F2 - D1	-759.8237651	< 0.001	< 0.001	***
D2 - D1	-113.3951051	< 0.001	< 0.001	***
E3 - D1	371.2860167	< 0.001	< 0.001	***
G3 - E1	0.1529475	1	0.429	
E2 - E1	0.6271855	1	0.265	
G1 - E1	-2.3193792	< 0.001	< 0.001	***
E4 - E1	-0.8747398	1	0.191	
F2 - E1	-4.0529123	< 0.001	< 0.001	***
D2 - E1	-3.7058180	< 0.001	< 0.001	***
E3 - E1	1.6099742	1	0.053	
D1 - E1	-0.3400350	1	0.367	
G3 - D4	104.5580843	< 0.001	< 0.001	***
E2 - D4	101.1075288	< 0.001	< 0.001	***
G1 - D4	60.3152193	< 0.001	< 0.001	***
E4 - D4	145.0436499	< 0.001	< 0.001	***
F2 - D4	26.8714577	< 0.001	< 0.001	***
D2 - D4	15.5317820	< 0.001	< 0.001	***
E3 - D4	1238.2207443	< 0.001	< 0.001	***
D1 - D4	720.0861501	< 0.001	< 0.001	***
E1 - D4	4.1671052	< 0.001	< 0.001	***

Tab.7 Dunn's Test pairwise comparison of **Nitrogen exceedance** by EUNIS level 2 habitat categories

PAIRWISE COMPARISON	Z- STATISTIC	P.ADJUSTED	P	
G3 - F2	8.665522e+00	< 0.001	< 0.001	***
G3 - E2	6.342006e+01	< 0.001	< 0.001	***
F2 - E2	4.796903e+01	< 0.001	< 0.001	***
G3 - G1	6.917245e+01	< 0.001	< 0.001	***
F2 - G1	5.148837e+01	< 0.001	< 0.001	***
E2 - G1	4.474699e-02	1	0.482	
G3 - E4	8.954897e+01	< 0.001	< 0.001	***
F2 - E4	6.637707e+01	< 0.001	< 0.001	***
E2 - E4	1.485313e+01	< 0.001	< 0.001	***
G1 - E4	1.991168e+01	< 0.001	< 0.001	***
G3 - E1	7.254315e+01	< 0.001	< 0.001	***
F2 - E1	5.607943e+01	< 0.001	< 0.001	***
E2 - E1	1.021770e+01	< 0.001	< 0.001	***
G1 - E1	1.161041e+01	< 0.001	< 0.001	***
E4 - E1	-6.628828e-01	1	0.254	
G3 - E3	-2.631942e+01	< 0.001	< 0.001	***
F2 - E3	-3.433625e+01	< 0.001	< 0.001	***
E2 - E3	-1.420243e+02	< 0.001	< 0.001	***
G1 - E3	-1.908750e+02	< 0.001	< 0.001	***
E4 - E3	-1.149709e+03	< 0.001	< 0.001	***
E1 - E3	-1.603987e+02	< 0.001	< 0.001	***
G3 - D4	-3.011365e+00	0.0715	0.0013	
F2 - D4	-1.405573e+01	< 0.001	< 0.001	***
E2 - D4	-1.100753e+02	< 0.001	< 0.001	***
G1 - D4	-1.475475e+02	< 0.001	< 0.001	***
E4 - D4	-7.844593e+02	< 0.001	< 0.001	***
E1 - D4	-1.275180e+02	< 0.001	< 0.001	***
E3 - D4	1.838820e+02	< 0.001	< 0.001	***
G3 - D2	4.128607e+00	< 0.001	< 0.001	***
F2 - D2	3.541646e+00	0.01	0.0002	*
E2 - D2	6.370785e-01	1	0.262	
G1 - D2	6.354126e-01	1	0.263	
E4 - D2	1.503078e-01	1	0.44	
E1 - D2	1.713902e-01	1	0.432	
E3 - D2	5.304367e+00	< 0.001	< 0.001	***
D4 - D2	4.266945e+00	< 0.001	< 0.001	***
G3 - D1	8.884758e+01	< 0.001	< 0.001	***
F2 - D1	6.580260e+01	< 0.001	< 0.001	***
E2 - D1	1.402322e+01	< 0.001	< 0.001	***
G1 - D1	1.875953e+01	< 0.001	< 0.001	***
E4 - D1	-5.720634e+00	1	< 0.001	
E1 - D1	-1.551487e-01	1	0.438	
E3 - D1	1.022287e+03	< 0.001	< 0.001	***
D4 - D1	7.163799e+02	< 0.001	< 0.001	***
D2 - D1	-1.764425e-01	1	0.43	

Tab.8 Dunn's Test pairwise comparison of **risk of warming** by EUNIS level 2 habitat categories

PAIRWISE COMPARISON	Z- STATISTIC	P.ADJUSTED	P	
G3 - E2	-63.9273598	< 0.001	< 0.001	***
G3 - G1	-32.8964749	< 0.001	< 0.001	***
E2 - G1	41.1528683	< 0.001	< 0.001	***
G3 - E1	-102.6513200	< 0.001	< 0.001	***
E2 - E1	-16.0134188	< 0.001	< 0.001	***
G1 - E1	-82.6322839	< 0.001	< 0.001	***
G3 - E4	33.2943381	< 0.001	< 0.001	***
E2 - E4	114.4121630	< 0.001	< 0.001	***
G1 - E4	99.9695082	< 0.001	< 0.001	***
E1 - E4	274.2564910	< 0.001	< 0.001	***
G3 - F2	20.0461180	< 0.001	< 0.001	***
E2 - F2	90.3662074	< 0.001	< 0.001	***
G1 - F2	63.6012231	< 0.001	< 0.001	***
E1 - F2	157.0698073	< 0.001	< 0.001	***
E4 - F2	-12.0342580	< 0.001	< 0.001	***
G3 - D1	-41.0721507	< 0.001	< 0.001	***
E2 - D1	48.7845108	< 0.001	< 0.001	***
G1 - D1	-0.3568360	1	0.361	
E1 - D1	137.6355201	< 0.001	< 0.001	***
E4 - D1	-738.6460041	< 0.001	< 0.001	***
F2 - D1	-91.1649854	< 0.001	< 0.001	***
G3 - E3	27.7101760	< 0.001	< 0.001	***
E2 - E3	109.3101033	< 0.001	< 0.001	***
G1 - E3	92.0542482	< 0.001	< 0.001	***
E1 - E3	261.5957741	< 0.001	< 0.001	***
E4 - E3	-46.5988288	< 0.001	< 0.001	***
F2 - E3	4.3649141	< 0.001	< 0.001	***
D1 - E3	542.9200682	< 0.001	< 0.001	***
G3 - D4	2.0205625	1	0.022	
E2 - D4	6.4458410	< 0.001	< 0.001	***
G1 - D4	3.8963660	< 0.001	< 0.001	***
E1 - D4	7.3760064	< 0.001	< 0.001	***
E4 - D4	0.4937855	1	0.311	
F2 - D4	0.8910322	1	0.186	
D1 - D4	3.9107607	< 0.001	< 0.001	***
E3 - D4	0.7464207	1	0.228	
G3 - D2	37.4781853	< 0.001	< 0.001	***
E2 - D2	118.0246816	< 0.001	< 0.001	***
G1 - D2	105.4298492	< 0.001	< 0.001	***
E1 - D2	280.7959658	< 0.001	< 0.001	***
E4 - D2	41.2162493	< 0.001	< 0.001	***
F2 - D2	17.8700235	< 0.001	< 0.001	***
D1 - D2	697.5054473	< 0.001	< 0.001	***
E3 - D2	75.7683871	< 0.001	< 0.001	***
D4 - D2	-0.2994560	1	0.382	

Tab.9 Dunn’s Test pairwise comparison of **risk of drought** by EUNIS level 2 habitat categories

PAIRWISE COMPARISON	Z- STATISTIC	P.ADJUSTED	P	
G3 - F2	20.573421	< 0.001	< 0.001	***
G3 - G1	14.620617	< 0.001	< 0.001	***
F2 - G1	-9.562322	< 0.001	< 0.001	***
G3 - E2	-56.309993	< 0.001	< 0.001	***
F2 - E2	-75.221989	< 0.001	< 0.001	***
G1 - E2	-89.204652	< 0.001	< 0.001	***
G3 - E4	34.278483	< 0.001	< 0.001	***
F2 - E4	2.680180	< 0.001	< 0.001	***
G1 - E4	21.609666	< 0.001	< 0.001	***
E2 - E4	178.334850	< 0.001	< 0.001	***
G3 - E1	15.851097	< 0.001	< 0.001	***
F2 - E1	-8.707913	< 0.001	< 0.001	***
G1 - E1	1.247371	1	0.106	
E2 - E1	92.694666	< 0.001	< 0.001	***
E4 - E1	-20.601732	< 0.001	< 0.001	***
G3 - D1	38.069109	< 0.001	< 0.001	***
F2 - D1	6.023830	< 0.001	< 0.001	***
G1 - D1	26.702267	< 0.001	< 0.001	***
E2 - D1	184.621233	< 0.001	< 0.001	***
E4 - D1	37.916389	< 0.001	< 0.001	***
E1 - D1	25.878292	< 0.001	< 0.001	***
G3 - E3	44.147208	< 0.001	< 0.001	***
F2 - E3	11.393212	< 0.001	< 0.001	***
G1 - E3	34.849159	< 0.001	< 0.001	***
E2 - E3	194.558738	< 0.001	< 0.001	***
E4 - E3	84.467012	< 0.001	< 0.001	***
E1 - E3	34.316148	< 0.001	< 0.001	***
D1 - E3	48.471431	< 0.001	< 0.001	***
G3 - D4	-10.877430	< 0.001	< 0.001	***
F2 - D4	-12.468448	< 0.001	< 0.001	***
G1 - D4	-11.814149	< 0.001	< 0.001	***
E2 - D4	-7.605769	< 0.001	< 0.001	***
E4 - D4	-12.646749	< 0.001	< 0.001	***
E1 - D4	-11.880558	< 0.001	< 0.001	***
D1 - D4	-12.842928	< 0.001	< 0.001	***
E3 - D4	-13.158711	< 0.001	< 0.001	***
G3 - D2	40.142892	< 0.001	< 0.001	***
F2 - D2	7.842177	< 0.001	< 0.001	***
G1 - D2	29.484282	< 0.001	< 0.001	***
E2 - D2	188.264359	< 0.001	< 0.001	***
E4 - D2	57.442118	< 0.001	< 0.001	***
E1 - D2	28.760394	< 0.001	< 0.001	***
D1 - D2	18.430455	< 0.001	< 0.001	***
E3 - D2	-31.714139	< 0.001	< 0.001	***
D4 - D2	12.949625	< 0.001	< 0.001	***

Tab.10 Percentage of area affected by total risk, risk of warming, drought and N exceedance 'in'side Natura 2000 protection sites and 'out'side according to different combinations of climate and deposition scenarios.

TIME	CLIMATE SCENARIO	N DEPOSITION SCENARIO	TOTAL RISK_OUT	TOTAL RISK_IN	TEMP RISK_OUT	TEMP RISK_IN	DROUGHT RISK_OUT	DROUGHT RISK_IN	N EXCEED_OUT	N EXCEED_IN
2010	**current**	**N2010**	57	34	2	2	18	10	51	28
2030	**RCP2.6**	**N2010**	58	35	5	4	15	9	51	28
2030	**RCP2.6**	**CLE2030**	50	32	5	4	15	10	40	23
2030	**RCP2.6**	**MFR2030**	34	23	5	4	13	8	23	13
2030	**RCP8.5**	**N2010**	60	38	7	7	20	12	51	28
2030	**RCP8.5**	**CLE2030**	53	34	7	7	20	12	40	23
2030	**RCP8.5**	**MFR2030**	38	27	7	7	17	11	23	13
2050	**RCP2.6**	**N2010**	58	35	6	5	12	8	51	28
2050	**RCP2.6**	**CLE2030**	49	32	6	5	13	9	40	23
2050	**RCP2.6**	**MFR2030**	34	23	6	5	11	8	23	13
2050	**RCP8.5**	**N2010**	62	40	11	10	14	11	51	28
2050	**RCP8.5**	**CLE2030**	52	36	11	10	14	11	40	23
2050	**RCP8.5**	**MFR2030**	38	29	11	10	13	11	23	13

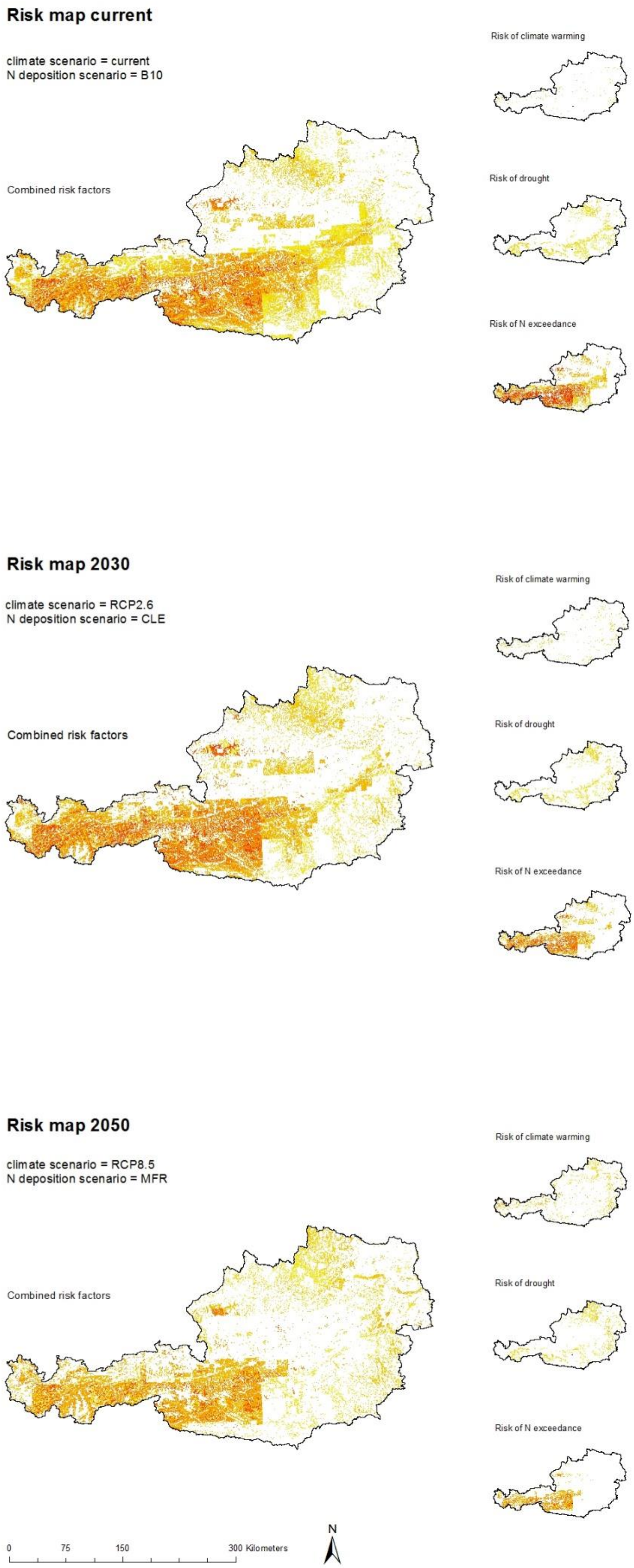

Fig.1 Risks maps of combined, N-, drought and warming risk for different scenario combinations.